High Resolution ^{1}H Nuclear Magnetic Resonance of a Transmembrane Peptide

James H. Davis,* Michèle Auger,‡ and Robert S. Hodges§
*Department of Physics, University of Guelph, Guelph, Ontario N1G 2W1; ‡Département de Chimie, Université Laval, Québec, Québec; and §Department of Biochemistry, University of Alberta, Edmonton, Alberta, Canada

ABSTRACT Although the strong ^{1}H-^{1}H dipolar interaction is known to result in severe homogeneous broadening of the ^{1}H nuclear magnetic resonance (NMR) spectra of ordered systems, in the fluid phase of biological and model membranes the rapid, axially symmetric reorientation of the molecules about the local bilayer normal projects the dipolar interaction onto the motional symmetry axis. Because the linewidth then scales as $(3\cos^2\theta - 1)/2$, where θ is the angle between the local bilayer normal and the magnetic field, the dipolar broadening has been reduced to an "inhomogeneous" broadening by the rapid axial reorientation. It is then possible to obtain high resolution ^{1}H-NMR spectra of membrane components by using magic angle spinning (MAS). Although the rapid axial reorientation effectively eliminates the homogeneous dipolar broadening, including that due to $n = 0$ rotational resonances, the linewidths observed in both lipids and peptides are dominated by low frequency motions. For small peptides the most likely slow motions are either a "wobble" or reorientation of the molecular diffusion axis relative to the local bilayer normal, or the reorientation of the local bilayer normal itself through surface undulations or lateral diffusion over the curved surface. These motions render the peptide ^{1}H-NMR lines too broad to be observed at low spinning speeds. However, the linewidths due to these slow motions are very sensitive to spinning rate, so that at higher speeds the lines become readily visible. The synthetic amphiphilic peptide $K_2GL_{20}K_2A$-amide (peptide-20) has been incorporated into bilayers of 1,2-di-d_{27}-myristoyl-*sn*-glycero-3-phosphocholine (DMPC-d_{54}) and studied by high speed ^{1}H-MAS-NMR. The linewidths observed for this transbilayer peptide, although too broad to be observable at spinning rates below ~5 kHz, are reduced to 68 Hz at a spinning speed of 14 kHz (at 50°C). Further improvements in spinning speed and modifications in sample composition designed to reduce the effectiveness of the slow motions responsible for the linewidth should result in significant further reduction in peptide linewidths. With this technique, there is now the potential for the use of ^{1}H-MAS-NMR for the study of conformation, folding, and dynamics of small membrane peptides and protein fragments.

INTRODUCTION

The cell's plasma membrane and all of its internal membranes have at least three characteristics in common: 1) they are heterogeneous mixtures of lipids and proteins; 2) they are dynamic systems with very complex molecular motions; and 3) both the basic structure itself and the molecular motions are highly anisotropic. These properties have severely limited the application of many standard techniques for the study of molecular structure and dynamics. For example, the membrane's bilayer structure is quasi-two-dimensional. Within the bilayer itself the molecular heterogeneity of the system leads to a large degree of positional disorder, whereas the anisotropy of this quasi-two-dimensional structure leads to a high degree of local orientational order. This is reminiscent of smectic liquid crystals, systems that exhibit properties intermediate between those of liquids and solids, having positional disorder in at least one dimension yet having orientational order in one or more dimensions.

It is possible, using reconstituted or model membrane systems, to reduce the compositional heterogeneity. However, the system remains highly disordered. In some instances, for example bacteriorhodopsin in the purple membrane of *Halobacterium halobium*, it has been possible to obtain enough two-dimensional order to perform electron scattering and diffraction experiments and to determine a medium resolution structure for membrane proteins (Henderson and Unwin, 1975; Henderson et al., 1990; Wang et al., 1993). In a few other cases, it has been possible to co-crystallize membrane protein and detergent (Deisenhofer and Michel, 1989; Cowan et al., 1992; Picot et al., 1994) and to obtain the protein structures by x-ray diffraction. However, these cases are still rare and there does not yet appear to be one reliable protocol for obtaining highly ordered membrane protein crystals in either two or three dimensions.

Spectroscopic techniques also encounter formidable difficulties when applied to membrane systems. The strongly orientation-dependent electric and magnetic interactions dominate the linewidths of the observed spectra in these highly anisotropic systems. For example, ^{1}H nuclear magnetic resonance (NMR), which has become a powerful alternative method for protein structure determination in solution (especially when combined with ^{15}N isotopic labeling), has not been applied to proteins in membranes, although some work on peptides, small proteins, and protein fragments in small micelles has been performed (Arseniev et al., 1986; Peters et al., 1992; Kohda and Khagaki, 1992; Zetta et al., 1990; Shon et al., 1991; Henry and Sykes, 1992;

Received for publication 28 March 1994 and in final form 24 July 1995.
Address reprint requests to Dr. James H. Davis, Department of Physics, University of Guelph, Guelph, Ontario N1G 2W1, Canada. Tel.: 519-824-4120; Fax: 519-836-9967; E-mail: jhd@physics.uoguelph.ca.

0006-3495/95/11/1917/00 $2.00

Pascal and Cross, 1992). Recently, it has been possible to study the structure and dynamics of fragments of bacteriorhodopsin solubilized in SDS micelles using two- and three-dimensional ^{15}N-^{1}H high resolution NMR techniques (Orekov et al., 1992, 1994; Pervushin et al., 1994).

Solid state NMR studies of model and biological membranes have provided a great deal of insight into the molecular structure, orientational order, dynamics, and phase equilibria of these complex anisotropic systems, largely through the use of isotopic labeling. A variety of magnetic nuclei have been used to study lipids, peptides, and proteins in membranes, including ^{2}H (Ulrich et al., 1992; Prosser et al., 1994; Prosser and Davis, 1994; Davis, 1983, 1991, 1993; Seelig and Seelig, 1980), ^{13}C (McDermott et al., 1994; Smith et al., 1994a, b; Smith et al., 1989; Langlais, 1994; Griffin, 1981), ^{15}N (Ketchem et al., 1993; Opella et al., 1987; Wu et al., 1994), and ^{31}P (Watts, 1988; Seelig, 1978; Griffin, 1981). For example, ^{2}H-NMR of isotopically labeled peptides and proteins has been used to determine bond orientations and to study side-chain and backbone dynamics (Prosser et al., 1994; Prosser and Davis, 1994; Ulrich et al., 1992). ^{15}N-NMR has been used to determine the orientation of peptide planes in gramicidin A within lipid bilayers (Ketchem et al., 1993). Both static and magic angle spinning (MAS) ^{13}C-NMR have been used widely to study the conformation and orientational order, dynamics, and phase behavior of pure and mixed lipid bilayers (Huang et al., 1993). Rapid spinning of the sample about the so-called "magic angle," together with strong ^{1}H decoupling, removes the strong orientation-dependent second rank tensor interactions such as the anisotropic part of the chemical shift and the dipole-dipole interaction, leaving the scalar parts of the chemical shift and the J-coupling (Griffin, 1981). The resolution attainable for ^{13}C-MAS-NMR is impressive, approaching that obtainable for solutions. Conformational and structural studies of membrane proteins and peptides have been performed using the technique of "rotational resonance," wherein the dipolar coupling between two isotopically enriched carbons is reintroduced by adjusting the spinning rate to match directly (or to match a submultiple of) the chemical shift difference between the two carbon nuclei (Creuzet et al., 1991; Thompson et al., 1992; McDermott et al., 1994; Peersen et al., 1992, Smith et al., 1994a, b; Langlais, 1994).

Until recently the potentially most powerful nuclear magnetic probe, ^{1}H, has seen little application to membranes. This is because the incomplete motional averaging of the strong ^{1}H-^{1}H homonuclear dipolar coupling in these anisotropic systems results in a very broad (up to ~40 kHz), largely featureless ^{1}H-NMR spectrum (MacKay, 1981; MacKay et al., 1983; Kimmich et al., 1983; Bloom et al., 1977; Wennerstrom, 1973). Careful analysis of the ^{1}H-NMR lineshapes of multilamellar dispersions has extracted some useful general information on the changes in dynamics and phase behavior of membranes. However, the detailed site-specific data available in principle from ^{1}H-NMR are masked by the strong dipolar coupling. Isotopic dilution of the ^{1}H nuclei by incorporation of 90% deuterium in the sample dramatically reduces the dipolar broadening and, when combined with magic angle spinning, is a very promising approach (McDermott et al., 1992; Zheng et al., 1993). However, this requires uniform isotopic enrichment of all components of the system studied. The combination of magic angle spinning and ^{1}H multiple-pulse line narrowing techniques (CRAMPS) has also yielded very promising results in ordered systems (Maciel et al., 1990).

It has long been known that to use MAS to remove the "homogeneous" line broadening due to homonuclear dipole-dipole interactions among abundant nuclei (like protons), it is necessary to spin the sample at a rate much larger than the homogeneous linewidth (Haeberlen and Waugh, 1968). Even in the membrane's fluid phase, this homogeneous broadening is of the order of 10 kHz (Wennerstrom, 1973; Bloom et al., 1977; MacKay, 1981); thus, one expects to have to spin at rates of 40 or 50 kHz to narrow effectively the ^{1}H resonances. This is well beyond the current capabilities of the technique. However, in 1987 Oldfield et al. (see also Forbes et al., 1988) showed that one could obtain relatively high resolution ^{1}H-NMR spectra of phospholipids in multilamellar lipid/water dispersions by MAS. This somewhat surprising result is due to the rapid axially symmetric reorientation of the phospholipids about the local bilayer normal. This motion, which has a correlation time typically of the order of 10^{-10} s in the fluid phase (Prosser et al., 1992), is rapid enough to project the homogeneous proton dipole-dipole interaction onto the axis of symmetry for the motion (the bilayer normal) (Wennerstrom, 1973; Bloom et al., 1977). The dipolar broadening then depends only on the orientation of the local bilayer normal relative to the magnetic field, scaling as $P_2(\cos\theta)$, where θ is the angle between the bilayer normal and the magnetic field. In this manner, the "homogeneous" dipolar broadening is converted into an "inhomogeneous" broadening much like the chemical shift anisotropy that dominates the linewidth of ^{13}C- and ^{31}P-NMR spectra of membranes. Magic angle spinning effectively narrows resonances that are inhomogeneously broadened, even if the spinning rate is less than the line broadening. In that case, one observes spinning sideband patterns that roughly mimic the static lineshape (Griffin et al., 1988).

The initial failure to observe the ^{1}H-MAS-NMR spectra of peptides incorporated into lipid bilayers was interpreted to be due to their slow axial diffusion. However, it has been found since that the synthetic amphiphilic peptides (Davis et al., 1983; Huschilt et al., 1985; Pauls et al., 1985; Prosser et al., 1992) and gramicidin (Datema et al., 1986; Prosser et al., 1994; Prosser and Davis, 1994; Davis, 1988; Macdonald and Seelig, 1988) that had been investigated at that time do diffuse sufficiently rapidly about the local bilayer normal, with correlation times in the range of 10^{-9} to 10^{-7} s. We present here the results of a ^{1}H-MAS-NMR study of a synthetic bilayer-spanning peptide incorporated into multilamellar dispersions of 1,2-dimyristoyl-*sn*-glycero-3-phosphocholine (DMPC) in excess $^{2}H_2O$. The early

failure to observe these spectra was simply because the samples were spun too slowly (in the 3- to 4-kHz range). This spinning speed was not too slow because the lines were homogeneously broadened but, rather, because there was an additional slow motion that severely broadened the resonances. In this situation, it is necessary either to reduce the effectiveness of the slow motion or to spin faster than the inverse of the correlation time for the slow motion. After a brief description of the experimental procedures and sample preparation, we will present a physical description of this effect, present our experimental results, and then make a comparison with the predictions of the theory of Haeberlen and Waugh (1968, 1969) (Maricq and Waugh, 1979; Suwelack et al., 1980; Long et al., 1994). Finally, we will discuss the potential for the application of high speed ^{1}H-MAS-NMR for the study of small peptides and protein fragments in membrane systems.

MATERIALS AND METHODS

1,2-di-d_{27}-myristoyl-*sn*-glycero-3 phosphocholine (DMPC-d_{54}) was synthesized following the procedure of Gupta et al. (1975). Peptide-20, $K_2GL_{20}K_2A$-amide, molecular weight of ~3400, was synthesized as described in Davis et al. (1983). 1-palmitoyl-2-oleoyl-*sn*-glycero-3-phosphocholine (POPC) was purchased from Avanti Polar Lipids (Alabaster, AL). All of the NMR samples were prepared by dissolving the components to be mixed in distilled methanol that was then removed by gentle rotary evaporation at room temperature. The samples were then placed under vacuum overnight (for at least 10 h) to remove the last traces of solvent. The concentration of peptide in the peptide-20/DMPC-d_{54} sample was 6 ± 0.3 mol%. After determining the dry weight of the mixture in each case, the samples were hydrated using an amount of ^2H_2O equal to 80% by weight of the dry mixture, whether for pure lipid or for lipid/peptide mixtures. The total dry weight of a sample was typically 40 mg. The samples were mixed carefully using a small, stainless steel stirring rod and then transferred into the 5-mm-diameter SiN rotors (Doty Scientific, Columbia, SC). The hydrated sample mixture was centrifuged gently into the bottom of the rotor, after which the lip of the rotor was wiped dry carefully and the "long" Vespel end caps (Doty Scientific) were inserted. With this procedure, there was no problem with water loss or with loose-end caps even when spinning at rates of up to 14.7 kHz or at a temperature of 60°C. A solution sample of peptide-20 in $C^2H_3O^2H$ (plus tetramethylsilane, TMS) was used for comparison with the bilayer samples. This sample was placed in the same rotor as that used for the bilayer samples, and the spectrum was obtained under the same conditions (but spinning at much lower speed). All chemical shifts are measured with respect to the chemical shift of TMS in the peptide-20/$C^2H_3O^2H$/TMS sample.

An advisable precaution, especially when samples are unbuffered as in this report, is to test all samples for lipid hydrolysis after the experiments. Accordingly, the samples were redissolved in methanol and analyzed by thin layer chromatography using a 58:35:5.6:1.6 $CHCl_3$:methanol:H_2O:NH_4OH solvent system. No traces of sample degradation were found. The NMR spectra were obtained using a home-built spectrometer operating at a ^{1}H Larmor frequency of 360.01 MHz (corresponding to a static magnetic field of 8.5 T). The MAS probe was built using a high speed 5-mm spinning assembly from Doty Scientific. The ^{1}H 90-degree pulse length was ~2.8 μs. In most cases, 2048 complex points were acquired using dwell times of either 100 or 200 μs. The recycle delay was typically 3.0 s, and 128 scans were collected. CYCLOPS phase cycling (Hoult and Richards, 1975) was used in all experiments.

The spinning assembly is completely enclosed by a copper oven whose temperature is controlled to within better than 0.1°C. The dry air, from a Balston Filter Products (Lexington, MA) air dryer, operating at pressures up to 80 lb/in^2, used for both bearing and turbine drive, was also temperature-controlled so that the temperature of the exit air (measured ~1 cm below the sample coil) and of the oven were equal. To test for effects of internal heating of the sample at high spinning speeds, a sample of DPPC/^2H_2O (Avanti Polar Lipids) was placed in the SiN rotor and the gel/fluid phase transition temperature was monitored as a function of sample spinning speed. The ^{1}H-NMR spectrum is very sensitive to the gel/fluid transition temperature because the axially symmetric reorientation, which permits the observation of the high resolution spectrum in the fluid phase, is dramatically slowed down in the gel phase. Thus, at the phase transition into the gel phase the ^{1}H-NMR spectrum broadens to the point of being essentially unobservable. Through this procedure, it was determined that under the conditions used in these experiments there was very little internal heating of the samples. The phase transition temperature of DPPC being within 2–3°C of its normal value (41°C) even at 14 kHz.

Theoretical background

The dipolar interaction between like spins

The orientation-dependent interactions responsible for the linewidths of the NMR spectra of partially (or completely) ordered systems such as membranes, liquid crystals, and solids depend on orientation relative to the magnetic field in a very simple way (we will restrict the discussion to the second rank tensor interactions such as the dipole-dipole interaction, the anisotropic part of the chemical shift, the first order quadrupolar interaction, etc.). As we will see, these interactions vary essentially as $(3\cos^2\beta - 1)/2$, where β is the angle between the interaction tensor's principal direction and the external magnetic field, H_0 (in the case where there is rapid axially symmetric reorientation, β is the angle between the axis of symmetry for the motion and the magnetic field). There is one particular angle, called the "magic" angle, where the value of $(3\cos^2\beta - 1)/2$ is zero, i.e., at $\beta_m = 54.7$.

For the case of the dipole-dipole interaction between two neighboring nuclei, having magnetic moments $\vec{\mu}_1 = \gamma_1\hbar\vec{I}_1$ and $\vec{\mu}_2 = \gamma_2\hbar\vec{I}_1$, the total Hamiltonian describing the system consists of two terms, the Zeeman Hamiltonian and the dipole-dipole Hamiltonian:

$$\begin{aligned}\mathcal{H} &= \mathcal{H}_Z + \mathcal{H}_D \\ &= -\gamma_1\hbar H_0 I_z - \gamma_2\hbar H_0 I_z \\ &\quad + \frac{\gamma_1\gamma_2\hbar}{r_{12}^3}[\vec{I}_1 \cdot \vec{I}_2 - 3(\vec{I}_1 \cdot \hat{r}_{12})(\vec{I}_2 \cdot \hat{r}_{12})],\end{aligned} \tag{1}$$

where $\hat{r}_{12} = \vec{r}_{12}/r_{12}$ is a unit vector directed along the vector joining the two nuclei, r_{12} is the distance between the two nuclei, and γ_1 and γ_2 are their nuclear gyromagnetic ratios, both equal to γ^1H for dipolar-coupled ^{1}H. Defining the principal axis system ($X_PY_PZ_P$) with its Z_P-axis aligned along the vector joining the two nuclei, the principal values of the dipolar tensor are

$$\mathcal{F}^P_{2,0} = -\sqrt{6}\,\gamma_{1H}^2\hbar/r_{12}^3 \qquad \mathcal{F}^P_{2,\pm1} = 0 \qquad \mathcal{F}^P_{2,\pm2} = 0. \tag{2}$$

We can write the interaction Hamiltonian in terms of its spatial and spin parts as

$$\mathcal{H}_D = \sum_{m=-2}^{+2} (-1)^m \mathcal{T}_{2,m}\mathcal{F}^L_{2,-m}. \tag{3}$$

The spatial part is described in the laboratory frame by

$$\mathcal{F}^L_{2,m} = \sum_{m'=-2}^{+2} \mathcal{F}^P_{2,m'}\mathcal{D}^{(2)}_{m',m}(\alpha_{PL}\beta_{PL}\gamma_{PL}), \tag{4}$$

where $\mathcal{D}^{(2)}(\alpha_{PL}\beta_{PL}\gamma_{PL})$ is the Wigner rotation matrix describing the transformation from the dipolar tensor principal axis system ($X_PY_PZ_P$) to the

laboratory coordinate system ($X_L Y_L Z_L$). The angles ($\alpha_{PL}\beta_{PL}\gamma_{PL}$) are the Euler angles for the transformation (Brink and Satchler, 1993; Zare, 1988). Because of the symmetry of the dipolar tensor in its principal axis system, we can take the third Euler angle (α_{PL}) to be zero:

$$\mathcal{F}^{L}_{2,0} = \mathcal{F}^{P}_{2,0}\mathcal{D}^{(2)}_{00}(0\beta_{PL}\gamma_{PL}) = \sqrt{\frac{3}{2}}\frac{\gamma_{1H}^2\hbar}{r_{12}^3}(3\cos^2\beta_{PL} - 1)$$

$$\mathcal{F}^{L}_{2,\pm1} = \mathcal{F}^{P}_{2,0}\mathcal{D}^{(2)}_{0\pm1}(0\beta_{PL}\gamma_{PL})$$

$$= \pm 3\frac{\gamma_{1H}\hbar}{r_{12}^3}\sin\beta_{PL}\cos\beta_{PL}\exp(\mp i\gamma_{PL}) \quad (5)$$

$$\mathcal{F}^{L}_{2,\pm2} = \mathcal{F}^{P}_{2,0}\mathcal{D}^{(2)}_{0\pm2}(0\beta_{PL}\gamma_{PL})$$

$$= -\frac{3}{2}\frac{\gamma_{1H}^2\hbar}{r_{12}^3}\sin^2\beta_{PL}\exp(\mp 2i\gamma_{PL}).$$

The spin-dependent part is given by

$$\mathcal{T}_{2,0}(I_1I_2) = \frac{1}{\sqrt{6}}[3I_{1z}I_{2z} - \vec{I}_1 \cdot \vec{I}_2]$$

$$\mathcal{T}_{2,\pm1}(I_1I_2) = \mp\frac{1}{2}[I_1^{\pm}I_{2z} + I_{1z}I_2^{\pm}] \quad (6)$$

$$\mathcal{T}_{2,\pm2}(I_1I_2) = \frac{1}{2}I_1^{\pm}I_2^{\pm}.$$

At high magnetic fields, the Zeeman Hamiltonian is much larger than the dipolar Hamiltonian; for example, at 8.5 T, the ^{1}H Larmor frequency is ~360 MHz whereas the dipolar coupling between the two geminal ^{1}H nuclei in a methylene group is of the order of 40 kHz. Thus, we can treat the dipolar interaction as a small perturbation on the Zeeman interaction and, therefore, in calculating spectra we only need to keep that part of the dipolar Hamiltonian that commutes with the Zeeman Hamiltonian. This so-called "secular" dipolar Hamiltonian is

$$\mathcal{H}'_d = \mathcal{F}^{L}_{2,0}\mathcal{T}_{2,0}(I_1I_2) \quad (7)$$

$$= -\frac{\gamma_1\gamma_2\hbar}{r_{12}^3}\frac{1}{2}(3\cos^2\beta_{PL} - 1)[3I_{1z}I_{2z} - \vec{I}_1 \cdot \vec{I}_2].$$

It is evident that if the sample is oriented so that the angle between the vector joining these two nuclei and the magnetic field vector is β_m, then the dipole-dipole interaction will be zero and the NMR spectrum will show no dipolar broadening. In a more complex system, where there may be many interacting nuclei, it will not be possible in general to orient the system so that all internuclear vectors make the same angle with respect to the magnetic field.

In membranes the molecular motions are highly anisotropic, so the orientation-dependent interactions are not averaged to zero. However, the local bilayer normal is an axis of symmetry for the motions in the fluid or liquid crystalline phase of membranes. If we introduce an "intermediate" reference frame ($X_N Y_N Z_N$), in this case with its Z_N-axis aligned along the local bilayer normal, then we need two Wigner rotation matrices and two sets of Euler angles to perform the successive transformations from principal axis to intermediate to laboratory frames. Using ($\alpha_{PN}\beta_{PN}\gamma_{PN}$) as the first set, for the transformation from principal axis to intermediate frame, and ($\alpha_{NL}\beta_{NL}\gamma_{NL}$) for the transformation from intermediate to laboratory frame, then successively,

$$\mathcal{F}^{N}_{2,m'} = \mathcal{F}^{P}_{2,0}\mathcal{D}^{(2)}_{0m'}(0\beta_{PN}\gamma_{PN}) \quad (8)$$

and

$$\mathcal{F}^{L}_{2,m} = \sum_{m'=-2}^{+2}\mathcal{F}^{N}_{2,m'}\mathcal{D}^{(2)}_{m'm}(\alpha_{NL}\beta_{NL}\gamma_{NL}). \quad (9)$$

Again, keeping only the "secular" part of the dipolar Hamiltonian, i.e., the terms in $T_{2,0}(I_1I_2)$, we obtain

$$\mathcal{H}_d = \mathcal{T}_{2,0}(I_1I_2)\sum_{m'}\mathcal{F}^{P}_{2,0}\mathcal{D}^{(2)}_{0m'}(0\beta_{PN}(t)\gamma_{PN}(t))\mathcal{D}^{(2)}_{m'0}(\alpha_{NL}\beta_{NL}0). \quad (10)$$

Here we have explicitly displayed the time dependence of the Euler angles ($0\beta_{PN}(t)\gamma_{PN}(t)$), which arises because of molecular reorientation with respect to the bilayer normal. The spectrum that we observe will be an average over some spectroscopic time scale. Thus, for the case of axially symmetric reorientation about the bilayer normal, where the time dependence of the angle γ_{PN} averages out all of the terms except that with $m' = 0$, the effective averaged dipolar Hamiltonian is

$$\langle\mathcal{H}_d\rangle = \mathcal{T}_{2,0}(I_1I_2)\mathcal{F}^{P}_{2,0}\langle d^{(2)}_{00}(\beta_{PN}(t))\rangle d^{(2)}_{00}(\beta_{NL})$$

$$= -\frac{\gamma_{1H}^2\hbar}{r_{12}^3}\frac{1}{2}\langle 3\cos^2\beta_{PN}(t) - 1\rangle \quad (11)$$

$$\cdot\frac{1}{2}(3\cos^2\beta_{NL} - 1)[3I_{1z}I_{2z} - \vec{I}_1 \cdot \vec{I}_2],$$

where the $d^{(2)}(\beta)$ are the reduced rotation matrices (Brink and Satchler, 1993; Zare, 1988). Then, defining $S_{HH} = \frac{1}{2}\langle 3\cos^2\beta_{PN} - 1\rangle$, we have

$$\langle\mathcal{H}_d\rangle = -\frac{\gamma_{1H}^2\hbar}{r_{12}^3}\frac{1}{2}(3\cos^2\beta_{NL} - 1)[3I_{1z}I_{2z} - \vec{I}_1 \cdot \vec{I}_2]S_{HH}, \quad (12)$$

where β_{NL} is the angle between the local bilayer normal and the static magnetic field. Thus, if one can prepare an oriented sample, for example, by depositing multilamellae on thin glass plates, so that the local bilayer normal is everywhere parallel to the normal to the plates, then by varying the orientation of the plates relative to the magnetic field, one can observe the $(3\cos^2\beta_{NL} - 1)/2$ dependence of the linewidths on orientation (Pope and Cornell, 1979; van der Leeuw et al., 1981; Sanders, 1993). In principle, orienting the glass plates with the normal at the magic angle relative to the magnetic field would produce a high resolution ^{1}H-NMR spectrum, with no dipolar broadening. Unfortunately, it has not been possible to obtain sufficient resolution by this method.

Magic angle spinning and the average Hamiltonian

The rapid axially symmetric reorientation of the phospholipids about the local bilayer normal projects the dipole-dipole interaction onto the axis of motional symmetry. In the same fashion, rapid rotation of a solid sample (with no internal motion) about an axis aligned at an angle β with respect to the magnetic field projects the complex dipole-dipole interactions onto the rotation axis. As in Eq. 12, the dipole-dipole Hamiltonian will scale as $(3\cos^2\beta - 1)/2$ so that at the magic angle, β_m, the dipole-dipole interaction is effectively averaged to zero. Thus, one can obtain in principle the high resolution ^{1}H-NMR spectrum of a solid or ordered sample simply by rotating the sample sufficiently rapidly at the magic angle. The fundamental question or problem is: How fast is necessary?

The physical rotation of the sample about an axis, called the rotor axis, inclined at some angle relative to $\vec{H}_0$, introduces an explicit periodic time dependence into the Hamiltonian, with period $\tau_R = 2\pi/\omega_R$. The basic idea of average Hamiltonian theory is that, for an experiment for which the Hamiltonian is made to be periodic in time, the evolution of the spin system

over one complete period can be described or calculated using an "average Hamiltonian." If we are only interested in the state of the spin system at the end of any integral number of periods (i.e., at $t = 0, \tau_R, 2\tau_R, \cdots n\tau_R \cdots$), and not in its detailed evolution in between these times, we can replace the true time-dependent Hamiltonian by the average Hamiltonian (Haeberlen and Waugh, 1968, 1969; Maricq and Waugh, 1979). This average Hamiltonian, $\bar{\mathcal{H}}$ can be expanded in an infinite series:

$$\bar{\mathcal{H}} = \sum_{\mu=0}^{\infty} \bar{\mathcal{H}}_\mu, \tag{13}$$

where the successive terms are

$$\bar{\mathcal{H}}_0 = \frac{1}{\tau_R}\int_0^{\tau_R} \mathcal{H}(t)\, dt,$$

$$\bar{\mathcal{H}}_1 = \frac{-i}{2\tau_R}\int_0^{\tau_R} dt \int_0^t dt'[\mathcal{H}(t), \mathcal{H}(t')],$$

and (14)

$$\bar{\mathcal{H}}_2 = \frac{-1}{6\tau_R}\int_0^{\tau_R} dt \int_0^t dt' \int_0^{t'} dt''\{[\mathcal{H}(t), [\mathcal{H}(t'), \mathcal{H}(t'')]] + [\mathcal{H}(t''), [\mathcal{H}(t'), \mathcal{H}(t)]]\}.$$

Here, the commutators $[\mathcal{H}(t), \mathcal{H}(t')] = \mathcal{H}(t)\mathcal{H}(t') - \mathcal{H}(t')\mathcal{H}(t)$, etc., involve the Hamiltonian at a time "t" with itself at a different time "t'." If the Hamiltonian commutes with itself at all times, the so-called "inhomogeneous" broadening case, then the only nonzero term in the expansion of the average Hamiltonian is the term $\bar{\mathcal{H}}_0$. This is the case, for example, when the NMR linewidth is due to the anisotropic chemical shift interaction (as for natural abundance ^{13}C). In the case of dipole-dipole interactions between many like spins, we can generalize the two-spin Hamiltonian of Eq. 10 to the interaction of spin "i" with all of its neighboring spins:

$$\mathcal{H}_d^i = -\gamma_{1_H}^2 \hbar \sum_{j\neq i} [3I_{iz}I_{jz} - \vec{I}_i \cdot \vec{I}_j]\zeta^{i,j}(t), \tag{15}$$

where the orientation- and time-dependent factor $\zeta^{i,j}(t)$ is defined by

$$\zeta^{i,j}(t) = \frac{1}{r_{ij}^3}\sum_{m'} \mathcal{D}^{(2)}_{0m'}(0\beta_{PR}\gamma_{PR})\mathcal{D}^{(2)}_{m'0}(\alpha_{RL}(t)\beta_{RL}0) \tag{16}$$

and where the intermediate frame, now labeled "R," refers to the "rotor" frame. Here we have shown explicitly the time dependence of the Euler angle $\alpha_{RL}(t)$ describing the rotation of the sample-fixed rotor frame whose Z_R axis defines the rotation axis of the sample. Because the sample rotation is of fixed frequency ω_R, we can write $\alpha_{RL}(t) = \omega_R t$. If there are at least three interacting spins, and they do not all lie on the same straight line, then this dipolar Hamiltonian does not commute with itself at different times, i.e.,

$$\begin{aligned}[\mathcal{H}_d^i(t), \mathcal{H}_d^i(t')] &= -\gamma_{1_H}^4\hbar^2 \sum_{j\neq i}\sum_{k\neq i} \zeta^{i,j}(t)\zeta^{i,k}(t')([3I_{iz}I_{jz}, \vec{I}_i \cdot \vec{I}_k] \\ &\quad - [3I_{iz}I_{kz}, \vec{I}_i \cdot \vec{I}_j] - [\vec{I}_i \cdot \vec{I}_j, \vec{I}_i \cdot \vec{I}_k]) \\ &= -\frac{1}{2}\gamma_{1_H}^4\hbar^2 \sum_{j\neq i}\sum_{k\neq i} \mathcal{C}^i_{j,k}\{\zeta^{i,j}(t)\zeta^{i,k}(t') - \zeta^{i,k}(t)\zeta^{i,j}(t')\},\end{aligned} \tag{17}$$

where, we have made use of the fact that $\mathcal{C}^i_{j,k} = -\mathcal{C}^i_{k,j}$. Thus, the Hamiltonian for dipole-dipole interactions among many like spins, for a rotating sample, will commute with itself at all times if and only if

$$\zeta^{i,j}(t)\zeta^{i,k}(t') = \zeta^{i,k}(t)\zeta^{i,j}(t') \tag{18}$$

for all t and t'. For a single pair of spins, or for a number of spins lying along a straight line (Eq. 18) will hold. In general, however, it is necessary to consider all of the higher order terms in the expansion of the average Hamiltonian (Eq. 14).

As the rotation period, τ_R, becomes short relative to the inverse of the "static" linewidth, i.e., relative to the linewidth, $1/T_2^{st}$, for a nonrotating sample, the higher order terms, $\bar{\mathcal{H}}_1, \bar{\mathcal{H}}_2, \cdots$ in the average Hamiltonian, become less and less important. For very short τ_R, one would only need to consider the zero-order term $\bar{\mathcal{H}}_0$. In this case, the averaging over the angle $\alpha_R(t)$ eliminates all terms with $m' \neq 0$ from the expression for the zero-order average Hamiltonian, because $\langle e^{-im'\omega_R t}\rangle_{\tau_R} = 0$ in Eq. 16. Thus, rapid rotation of the sample results in an average Hamiltonian that scales as $(3\cos^2\beta_{RL} - 1)/2$, and if $\beta_{RL} = \beta_m$, there will be no dipolar broadening in the spectrum obtained from sampling at $t = 0, \tau_R, 2\tau_R, \cdots, n\tau_R \cdots$. This defines what is meant by "rapid" rotation; it must be fast enough so that higher order terms in the average Hamiltonian are unimportant.

How fast is necessary? This is quite easy to estimate. If the ^1H-^1H dipolar interaction is primarily responsible for the width of the ^1H-NMR spectrum of a static sample, then we can obtain the mean-squared strength of the ^1H-^1H dipolar interaction from the second moment of the static ^1H spectrum:

$$M_2 = \int_{-\infty}^{\infty} \omega^2 f(\omega)\, d\omega, \tag{19}$$

where $f(\omega)$ is the experimental spectrum (normalized to unit area) and ω is the frequency in rad/s. For membrane systems, either with or without membrane proteins, the experimental rigid lattice second moment is $\sim 1.7 \times 10^{10}$ s^{-2} (MacKay, 1981; MacKay et al., 1983; Kimmich et al., 1983). Thus, we can consider a rotational motion, with correlation time τ_c, to be fast if $M_2\tau_c^2 \ll 1$ or, in the membrane case, if $\tau_c \ll 7.7 \times 10^{-6}$ s. Then, for uniform rotation with period $\tau_R = 2\pi \times \tau_c$, the rotation is fast if $\tau_R \ll 4.8 \times 10^{-5}$ s, corresponding to a rotation rate of $\nu_R \gg 21$ kHz.

What sort of line narrowing can we expect if we spin such a sample at a rate of 21 kHz? The term in $\bar{\mathcal{H}}_0$ makes no contribution to the linewidth. The contribution due to the term in $\bar{\mathcal{H}}_n$ is approximately (Haeberlen and Waugh, 1968):

$$k_n = \frac{1}{(n+1)!\cdot T_2^{st}} \times \left(\frac{\tau_R}{T_2^{st}}\right)^n. \tag{20}$$

On summing over all "n" we find a reduction in linewidth that is of the order of 30% (or larger, depending in detail on the form of the higher order terms). Such a small reduction is of little use because we require a reduction by a factor of 1000 or more to obtain high resolution ^1H spectra (a static linewidth of several tens of kHz must be reduced to a few Hz). Furthermore, an increase in spinning rate by another factor of 10 (to an unrealistic 210 kHz) reduces the contribution of the term in $\bar{\mathcal{H}}_1$ by only another factor of 10. Thus, spinning more rapidly accomplishes little in the case of "homogeneous" broadening. The current state of the art in MAS probe design is much too slow to allow the elimination of purely homogeneous line broadening for abundant ^1H in ordered systems.

The effect of axially symmetric molecular reorientation

If the molecules in the membrane undergo rapid axial reorientation about the bilayer normal, with a correlation time $\tau_c \ll T_2^{st}$, then the dipolar interaction is projected onto the bilayer normal as discussed earlier. Although it has not been possible to obtain high resolution ^1H-NMR spectra

using oriented multibilayers, it is possible to achieve high resolution with ^{1}H MAS. We can see in detail how this will work if we combine the four reference frames used in the earlier discussion.

We begin in the dipolar tensor's principal axis system, P, fixed at a particular nucleus "i". We then perform three successive transformations. First, from P to N, the bilayer normal system, we use Euler angles $(0\beta^{i,j}_{PN}\gamma^{i,j}_{PN}(t))$. Here we assume that the angle $\beta^{i,j}_{PN}$ between the vector $\vec{r}_{ij}$ and the bilayer normal, $\hat{N}$, is fixed, but that the molecule undergoes axial diffusion about $\hat{N}$, leading to the time dependence of $\gamma^{i,j}_{PN}$. Second, we perform the transformation from the bilayer fixed system, with Z_N-axis along $\hat{N}$, to the rotor-fixed system, with Z_R along the rotor axis. The Euler angles for this transformation, $(\alpha_{NR}\beta_{NR}\,0)$, are constant because the sample is assumed to be fixed within the rotor. Although these angles will vary from place to place within a "powder" sample as the orientation of the local bilayer normal varies, for calculating the dipole-dipole Hamiltonian for a particular spin "i" there is a well defined local axis of symmetry for the motion. When calculating the total "powder average" we need to vary these angles, but for each local region of the sample we obtain identical results. Finally, we perform the transformation from the rotor fixed axis to the laboratory frame, with Euler angles $(\alpha_{RL}(\tau)\beta_{RL}0)$. Here β_{RL} is the angle between the rotor axis and $\vec{H}_0$, and will be set at the magic angle. The rotation, as before, is at a fixed rate ω_R such that $\alpha_{RL}(\tau) = \omega_R\tau$. We use the time variable τ here to distinguish it from "t," which is used to describe the much shorter timescale variations in $\gamma^{i,j}_{PN}(t)$.

With these definitions, the dipolar tensor in the laboratory frame is

$$\mathcal{F}^{L}_{2,m} = \sum_{m'}\sum_{m''} \mathcal{F}^{P}_{2,0}\mathcal{D}^{(2)}_{0m''}(0\beta^{i,j}_{PN}\gamma^{i,j}_{PN}(t)) \cdot \mathcal{D}^{(2)}_{m''m'}(\alpha_{NR}\beta_{NR}0)\mathcal{D}^{(2)}_{m'm}(\alpha_{RL}(\tau)\beta_{RL}0). \tag{21}$$

If the axial molecular reorientation in $\gamma^{i,j}_{PN}$ is sufficiently fast, we can replace $\mathcal{D}^{(2)}_{0m''}(0\beta^{i,m}_{PN}\gamma^{i,m}_{PN}(t)) = e^{-im''\gamma^{i,j}_{PN}(t)}d^{(2)}_{0m''}(\beta^{i,m}_{PN})$ by its average over the motion. Then, because $\langle e^{-im''\gamma^{i,j}_{PN}(t)}\rangle_t = 0$, for $t \gg \tau_c$, the correlation time for the molecular reorientation about the bilayer normal, all terms in $m'' \neq 0$ will be averaged to zero, leaving only $m'' = 0$. Then, keeping only the secular part, the dipolar Hamiltonian for spin "i" becomes

$$\mathcal{H}^{i}_{d}(\tau) = -\gamma^2_{1H}\hbar\sum_{j\neq i}[3I_{iz}I_{jz} - \vec{I}_i\cdot\vec{I}_j]\bar{\zeta}^{i,j}(\tau), \tag{22}$$

where

$$\bar{\zeta}^{i,j}(\tau) = \frac{1}{r^3_{ij}}d^{(2)}_{00}(\beta^{i,j}_{PN})\sum_{m'}d^{(2)}_{0m'}(\beta_{NR})d^{(2)}_{m'0}(\beta_{RL})e^{-im'\omega_R\tau} = \frac{1}{r^3_{ij}}d^{(2)}_{00}(\beta^{i,j}_{PN})\times g(\tau). \tag{23}$$

$\bar{\zeta}^{i,j}(\tau)$ can be factored into two parts, one that depends on (i, j) and one that depends on τ. Thus, on taking the commutators in evaluating the higher order terms in the expansion of the average Hamiltonian, one sees immediately that the products of the orientation-dependent factors

$$\bar{\zeta}^{i,j}(\tau)\bar{\zeta}^{i,k}(\tau') = \left[\frac{1}{r^3_{ij}}d^{(2)}_{00}(\beta^{i,j}_{PN})g(\tau)\right]\times\left[\frac{1}{r^3_{ik}}d^{(2)}_{00}(\beta^{i,k}_{PN})g(\tau')\right] = \bar{\zeta}^{i,j}(\tau')\bar{\zeta}^{i,k}(\tau) \tag{24}$$

are equal. Thus, the Hamiltonian $\mathcal{H}^{i}_{d}(\tau)$ commutes with itself at all times and we can ignore the higher order terms in the average Hamiltonian. Because $\bar{\mathcal{H}}_0 = 0$, if $\beta_{RL} = \beta_m$, we can observe a high resolution ^{1}H-NMR spectrum. The primary requirement is simply that the molecules within the membrane undergo axially symmetric reorientation with a correlation time $\tau_c \ll 7.7\times10^{-6}$ s.

Simultaneous anisotropic chemical shifts and dipolar coupling

When we have a dipole-dipole interaction between a pair of nuclei with anisotropic chemical shifts, the resulting Hamiltonian in the absence of molecular reorientation is homogeneous, as discussed by Maricq and Waugh (1979) and by Levitt et al. (1990). Although ^{1}H anisotropic chemical shifts are not studied widely, presumably because of the overwhelming dipole-dipole interactions present in ordered systems containing ^{1}H, the magnitude of the anisotropy is appreciable, being of the order of 6 ppm for methylene ^{1}H in malonic acid (Haeberlen, 1976). The previous discussion can be extended easily to this case by introducing two new principal axis reference frames, those of the chemical shift tensors of the two ^{1}H nuclei. The "hierarchy" of reference frames and the Euler angles for the transformations between them are illustrated nicely by Fig. 1 of Levitt et al. (1990). We use the same scheme here, replacing the "crystal fixed" frame (labeled "C" in Levitt et al.) by our bilayer fixed frame, labeled "N."

In their principal axis frames, the spherical chemical shift tensors for the two nuclei are

$$\mathcal{F}^{P,i}_{2,0} = \sqrt{3/2}\delta_i \qquad \mathcal{F}^{P,i}_{2,\pm1} = 0 \qquad \mathcal{F}^{P,i}_{2,\pm2} = -\tfrac{1}{2}\eta_i\delta_i \tag{25}$$

where $\delta_i = \sigma^i_{33} - \delta_{0i}$ is the chemical shift anisotropy, $\delta_{0i} = \mathrm{Tr}(\sigma^i)$ is the isotropic chemical shift of spin "i" and $\eta_i = (\sigma^i_{22} - \sigma^i_{11})/(\sigma^i_{33} - \delta_{0i})$ is the asymmetry parameter. The cartesian chemical shift tensors σ^i are defined such that their principal values obey the relations (Mehring, 1983; Griffin et al., 1988):

$$|\sigma^i_{33} - \delta_{0i}| \geq |\sigma^i_{11} - \delta_{0i}| \geq |\sigma^i_{22} - \delta_{0i}|. \tag{26}$$

Because of the very rapid axially symmetric reorientation of the leucine methyl groups about their C—C bonds, the methyl ^{1}H (spin I_1) chemical shift tensor can be replaced by a symmetric tensor with anisotropy $\delta'_1 = \delta_1/3$ (and with $\eta' = 0$).

The transformations from the three principal axis systems (for the chemical shift tensors of spin I_1 and of spin I_2, and the dipolar tensor of the combined system I_1I_2) to the bilayer fixed system "N" involve three different sets of Euler angles. Thus, in the N-frame,

$$\mathcal{F}^{N,I_1}_{2,m''} = \mathcal{F}^{P,I_1}_{2,0}\mathcal{D}^{(2)}_{0m''}(0\beta_{P_1N}\gamma_{P_1N})$$
$$\mathcal{F}^{N,I_2}_{2,m''} = \sum_{m'''}\mathcal{F}^{P,I_2}_{2,m'''}\mathcal{D}^{(2)}_{m'''m''}(\alpha_{P_2N}\beta_{P_2N}\gamma_{P_2N}) \tag{27}$$
$$\mathcal{F}^{N,I_1I_2}_{2,m''} = \mathcal{F}^{P,I_1I_2}_{2,0}\mathcal{D}^{(2)}_{0,m''}(0\beta_{P_1I_2N}\gamma_{P_1I_2N}).$$

The axially symmetric reorientation of the peptide about its long axis leads to the modulation of the angles γ_{PN}. Averaging each of these expressions over this fast motion gives expressions involving $\langle\exp[-im''\gamma_{PN}(t)]\rangle = 0$ if $m'' \neq 0$. Thus, we have after motional averaging

$$\mathcal{F}^{N,I_1}_{2,0} = \langle\mathcal{F}^{N,I_1}_{2,0}(t)\rangle_t = \mathcal{F}^{P,I_1}_{2,0}d^{(2)}_{00}(\beta_{P_1N})$$
$$\mathcal{F}^{N,I_2}_{2,0} = \sum_{m'''}\mathcal{F}^{P,I_2}_{2,m'''}e^{im'''\alpha_{P_1N}}d^{(2)}_{m'''0}(\beta_{P_2N}) \tag{28}$$
$$\mathcal{F}^{N,I_1I_2}_{2,0} = \mathcal{F}^{P,I_1I_2}_{20}d^{(2)}_{00}(\beta_{P_1I_2N}).$$

Next we transform from the local bilayer normal to the rotor-fixed frame R. As before (cf. discussion preceding Eq. 20), these angles will vary from place to place within the sample (i.e., from "crystallite" to "crystallite") and for a powder average we will need to average over them. For individual "crystallites," these angles are time-independent, however. Thus, all three tensors transform using the same angles so that in the rotor frame, they all will have the form

$$\mathcal{F}^{R}_{2,m'} = \mathcal{F}^{N}_{2,0}\mathcal{D}^{(2)}_{0m'}(0\beta_{NR}\gamma_{NR}). \tag{29}$$

The expressions for the three tensors in the rotor-fixed frame depend on the orientations of their principal axes systems with respect to the local bilayer normal and on the orientation of the normal with respect to the rotor axis. After the averaging over the rapid axially symmetric molecular reorientation, these tensor elements are independent of time on the much longer time scale, τ, associated with the spinning of the sample.

The transformation from the rotor fixed frame R to the laboratory frame is accomplished as before, with Euler angles $\alpha_{RL}(\tau)$ specifying the orientation of the rotor at time τ relative to its orientation at $\tau = 0$, and $\beta_{RL} = 54.7°$, the magic angle. Explicitly evaluating these transformations leads, as in Eq. 22, to (Maricq and Waugh, 1979; Griffin et al., 1988; Mehring, 1983):

$$\begin{aligned}\mathcal{F}^{L}_{20}(\tau) &= [C_2(\Omega_{NR})\cos 2\alpha_{RL}(\tau) + S_2(\Omega_{NR})\sin 2\alpha_{RL}(\tau) \\ &\quad + C_1(\Omega_{NR})\cos \alpha_{RL}(\tau) + S_1(\Omega_{NR})\sin \alpha_{RL}(\tau)]\mathcal{F}^{N}_{20} \\ &= g(\tau)\mathcal{F}^{N}_{20}, \end{aligned} \tag{30}$$

where $\Omega_{NR} = (0\beta_{NR}\gamma_{NR})$. All three tensors involve expressions of the same form, with the same τ-dependent factor $g(\tau)$. Restricting ourselves to the secular part of the Hamiltonian, we have

$$\begin{aligned}\mathcal{H}(\tau) &= \mathcal{F}^{I_1}_{00}\mathcal{T}_{00}(I_1) + \mathcal{F}^{I_2}_{00}\mathcal{T}_{00}(I_2) + \mathcal{F}^{L,I_1}_{20}(\tau)\mathcal{T}_{20}(I_1) \\ &\quad + \mathcal{F}^{L,I_2}_{20}(\tau)\mathcal{T}_{20}(I_2) + \mathcal{F}^{L,I_1I_2}(\tau)\mathcal{T}_{20}(I_1I_2) \\ &= k_1I_{1z} + k_2I_{2z} + g(\tau) \\ &\quad \times \{k_3[3I^2_{1z} - \vec{I}_1 \cdot \vec{I}_1] + k_4[3I^2_{2z} - \vec{I}_2 \cdot \vec{I}_2] \\ &\quad + k_5[3I_{1z}I_{2z} - \vec{I}_1 \cdot \vec{I}_2]\}. \end{aligned} \tag{31}$$

This Hamiltonian does not commute with itself at all times under all conditions. However, because all of the "τ" dependence is in the common term $g(\tau)$, we can identify easily the situations where it is not self-commuting.

Identical isotropic chemical shifts: $n = 0$ rotational resonance

If the spinning rate, ν_R, is such that

$$\Delta\nu_I = n \times \nu_R \tag{32}$$

when $\Delta\nu_I$ is the difference in isotropic chemical shifts of the two dipolar coupled nuclei, then we observe a dramatic broadening of the resonance lines (Maricq and Waugh, 1979; Raleigh et al., 1988; Levitt et al., 1990). This is the nth order rotational resonance condition. If we spin faster than the difference between any two isotropic chemical shifts in the system (in our case, this requires us to spin faster than ~3.6 kHz), then the only rotational resonance possible is for $n = 0$. This can occur (by Eq. 32) only when the two nuclei have identical isotropic chemical shifts (such as for two ^{1}H nuclei on a peptide leucine methyl group). Taking the commutator of the Hamiltonian in Eq. 31 with itself at two different times, τ_1 and τ_2, we have (Maricq and Waugh, 1979):

$$\begin{aligned}&[\mathcal{H}(\tau_1), \mathcal{H}(\tau_2)] \\ &\quad = -k_5[g(\tau_2) - g(\tau_1)](k_1[I_{1z}, \vec{I}_1 \cdot \vec{I}_2] + k_2[I_{2z}, \vec{I}_1 \cdot \vec{I}_2]) \\ &\quad = k_5[g(\tau_2) - g(\tau_1)][k_1 - k_2][i(I^+_1I^-_2 - I^-_1I^+_2)] \end{aligned} \tag{33}$$

Because k_1 and k_2 are the isotropic chemical shifts of the two nuclei (assumed to be equal), this Hamiltonian commutes with itself and we expect no contribution to the linewidth from an $n = 0$ rotational resonance condition. This is a direct result of the common axially symmetric motional averaging of the anisotropic chemical shift and dipolar tensors, which projects them all onto the same axis (the local bilayer normal). In a more general case, or in the absence of axially symmetric motion, we would expect an important contribution to the linewidth from $n = 0$ rotational resonance. As discussed by Maricq and Waugh (1979) and by Levitt et al. (1990), this contribution to the linewidth is expected to decrease roughly as $1/\nu_R$.

General case of nonequivalent nuclei

In the case where the two spins have different isotropic chemical shifts, we have no rotational resonances if we spin faster than 3 or 4 kHz. However, the Hamiltonian in Eq. 31 is still partly homogeneous because it does not commute with itself at all times. The first order correction to the zero-order average Hamiltonian involves the commutator of Eq. 32. Because in general $k_5 \neq 0$, $k_1 \neq k_2$, and $g(\tau_2) \neq g(\tau_1)$, this commutator is not zero. The magnitude of this correction term can be estimated from k_1, k_2, and k_5 and we expect a contribution to the linewidth that is of the order of (Maricq and Waugh, 1979; Levitt et al., 1990):

$$\Delta\nu_H \approx \frac{(k_1 - k_2)k_5}{\nu_R}. \tag{34}$$

It will turn out that this contribution, although significant, is quite small so that the predominant broadening mechanism must be due to slow motions. We will give a rough quantitative estimate of this homogeneous contribution to the linewidth in the discussion section.

The influence of intermediate time scale motions

That one can obtain high resolution ^{1}H-NMR MAS spectra of lipids in membranes was demonstrated in 1987 (Oldfield et al., 1987; Forbes et al., 1988). The correlation time for axial diffusion of lipids in the membrane fluid phase is of the order of 10^{-10} s, easily fast enough to project the dipole-dipole interactions onto the motional symmetry axis. The axial diffusion correlation times for peptides is significantly slower, having a value of $\sim 7 \times 10^{-9}$ s for gramicidin D in 1,2-lauroyl-*sn*-glycero-3-phosphocholine (DLPC) (Prosser et al., 1994), but still fast enough to effectively average the dipolar interactions. The difficulty in observing ^{1}H-MAS-NMR spectra for small peptides is due to the presence of other, slower motions that dominate the linewidths. Even the phospholipid spectra have linewidths of ~0.05 ppm (10–20 Hz at 360 MHz), again because of the presence of slow or intermediate time scale motions. ^{2}H-NMR relaxation studies of gramicidin D have identified what is probably the most significant cause of line broadening of the peptide's ^{1}H resonances. This is the "wobble" of the diffusion axis with respect to the local bilayer normal which, for that system, has a correlation time of $\sim 6 \times 10^{-6}$ s (Prosser et al., 1994; Prosser and Davis, 1994). The linewidth of a MAS resonance line, at a spinning rate ω_R, in the presence of a single intermediate time scale motion of correlation time τ_c is (Haeberlen and Waugh, 1969):

$$\frac{1}{T_2^{rot}} = \frac{1}{3\pi} \cdot \Delta M_2 \cdot \left\{\frac{2\tau_c}{1 + (\omega_R\tau_c)^2} + \frac{\tau_c}{1 + 4(\omega_R\tau_c)^2}\right\}, \tag{35}$$

where ΔM_2 is that part of the total dipolar second moment that is being modulated by the intermediate time scale motion. Thus, the modulation of the local dipolar fields by the sample rotation results in an enhanced sensitivity to internal local field fluctuations of comparable frequency. The significance of this contribution to the linewidth depends on two factors, the correlation time relative to the spinning rate and the fraction ΔM_2 of the interaction modulated by these motions. This may suggest some methods for eliminating, or at least minimizing, this important source of broadening.

RESULTS

The static and MAS ^{1}H-NMR spectra of a multilamellar dispersion of POPC/^2H_2O at 30°C are shown in Fig. 1 *a*, plotted on a scale of ±50 ppm (or ±18 kHz at the ^{1}H Larmor frequency of 360 MHz). The full width at half-maximum of the static spectrum is ~10 ppm, more than the entire isotropic chemical shift dispersion. The MAS ^{1}H spectrum of the same sample at the same temperature is shown under the broad static peak, and in expanded form in Fig. 1 *b*. The assignments for the different peaks have been published elsewhere (Oldfield et al., 1987; Forbes et al., 1988; Shan, 1990; Sparling et al., 1989). Although the spectrum in Fig. 1 *b* was taken at a rotation rate of 14 kHz, the linewidths are only slightly dependent on the speed of rotation, as shown in Fig. 2. The solid symbols give the linewidths for the peaks at 0.91 ppm (●, the chain methyls), 2.04 ppm (■, the CH_2 next to the oleoyl double bond), 3.25 ppm (◆, the choline γ-$(CH_3)_3$), and 3.69 ppm (▲, the choline β-CH_2) as a function of rotation rate. From 5 to 14 kHz, the linewidth of the chain methyls decreases by only ~10%, those of the other three peaks by ~30%. These linewidths, ranging from 13 to 34 Hz, correspond to T_2 values from 10 to 40 ms, which is in precise agreement with the low frequency ^{1}H T_1 values reported by Kimmich et al. (1983), for the range of frequencies from 10 to 100 kHz, for DPPC in its lamellar liquid crystalline phase at 45°C and above. Measurements of the ^{1}H spin lattice relaxation rates in the rotating frame (Shan, 1990; Le Guerneve and Auger, 1995), which are sensitive to local field fluctuations over this same frequency range, have yielded similar values, ranging, for example, from ~30 to 180 ms for different positions in DMPC in the fluid phase. These relaxation measurements have shown that the frequency dispersion of the spectral density in this frequency range is relatively flat so that, on the basis of the discussion in the previous section, not much variation with spinning rate is expected. We can expect little improvement in the linewidths for phospholipid dispersions unless a way is found to eliminate these low frequency fluctuations.

To minimize the overlapping of the lipid "solvent" resonances with the peptide-20 "solute" signals, the peptide-20/lipid mixtures used chain-perdeuterated DMPC-d_{54}. The ^{1}H-MAS spectrum of DMPC-d_{54} at 30°C, at a spinning rate of 8.0 kHz, is shown in Fig. 3 *a*. The chain resonances are

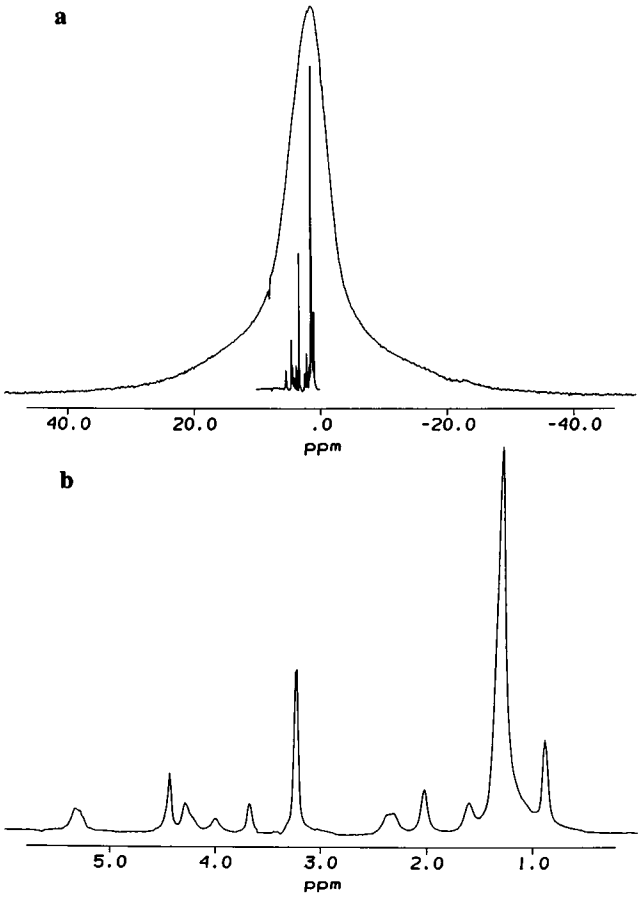

FIGURE 1 (*a*) The ^{1}H-NMR spectrum of a static (nonspinning) POPC/^2H_2O sample at 360.01 MHz at 30°C. On the same scale is shown the ^{1}H-MAS-NMR spectrum of the same sample, under the same conditions, except that it is rotating about the magic angle at a rate of 14 kHz. (*b*) The ^{1}H-MAS-NMR spectrum from part *a* of the figure, shown on an expanded horizontal scale. Chemical shifts are relative to TMS.

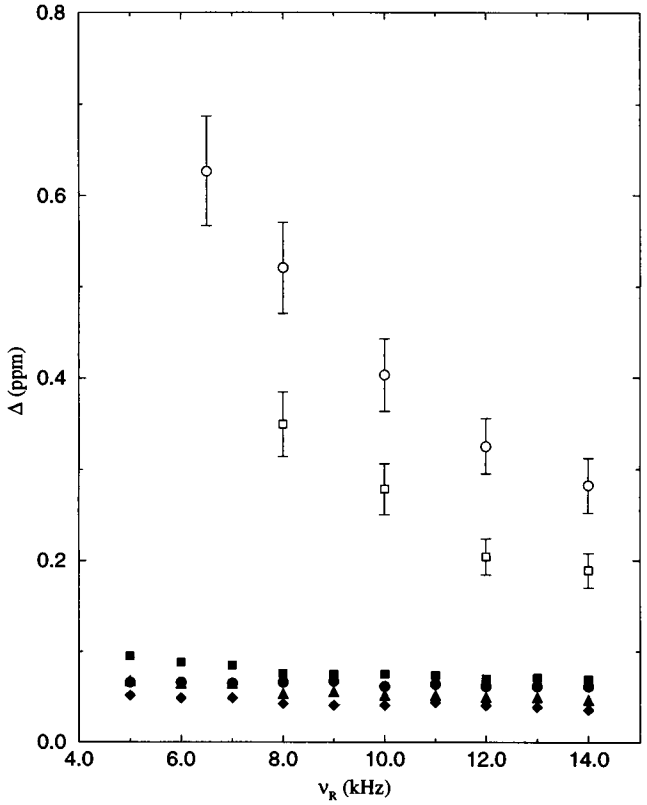

FIGURE 2 The linewidths, in ppm, as a function of spinning rate of selected peaks from the ^{1}H-MAS-NMR spectra at 360.01 MHz of POPC/^2H_2O: (◆) γ-$N(CH_3)_3$; (▲) β-CH_2; (●) chain methyls; (■) C^1H_2-C═C-C^1H_2- of *sn*-1-oleoyl chain and of the leucine methyl group peak from the peptide-20/DMPC-d_{54}/^2H_2O sample; (○) T = 30°C, and (□) T = 50°C.

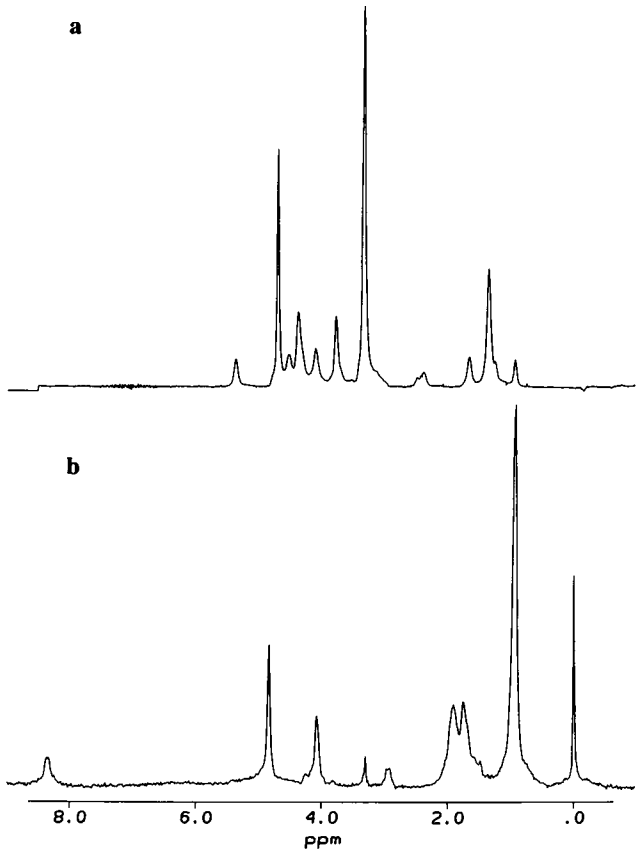

FIGURE 3 (*a*) The ^{1}H-MAS-NMR spectrum of DMPC-d_{54} at 30°C, spinning at a rate of 8.0 kHz. The chain resonances are reduced because of their (95%) deuteration. (*b*) The ^{1}H-NMR spectrum of peptide-20 in $C^2H_3O^2H$ with TMS at 30°C in the same rotor but spinning at ~1 kHz. All chemical shifts are relative to TMS from this sample. The peptide leucine methyl resonance is at 1.01 ppm, the two peaks near 1.8 and 1.9 ppm are from the leucine, and lysine methylenes, and methines, the peptide α-C^1Hs are near 4.05 ppm, and the unexchanged N-^{1}H are found near 8.3 ppm. The two peaks near 3.4 and 4.9 ppm are from residual ^{1}H in the solvent.

reduced greatly in amplitude as expected. For comparison, the spectrum of peptide-20 dissolved in $C^2H_3O^2H$, with TMS, is shown in Fig. 3 *b*. The large peak at ~1.0 ppm is from the leucine methyl groups, whereas the two peaks around 1.8–1.9 ppm are primarily due to the leucine methylenes and methines and the lysine methylenes. The small peak at 3.0 ppm is from the lysine ϵ-CH_2s, whereas that at ~4.0 ppm is from the ^{1}Hs on the peptide α-carbons, and the peak at 8.3 ppm is from the peptide N-Hs. Peptide-20 forms a very stable α-helix, even in solution at high temperatures (Davis et al., 1983); thus, there remains a large fraction of the amide ^{1}Hs that is unexchanged even in deuterated methanol. The peaks near 3.4 and 4.9 ppm are due to the solvent. By far the strongest peptide-20 resonance is for the leucine methyl groups, which lie almost directly under the strong lipid chain methyl and methylene resonances; thus, it is imperative to use fully deuterated lipids. Because of the large molecular weight difference between the peptide and the lipids, and of the necessity to ensure a well defined fluid bilayer phase, the peptide-20 comprised only 6 mol% of the lipid/peptide mixture; hence, the peptide resonances are expected to be small relative to the lipid's. The linewidths of this solution peptide-20 spectrum are quite large. For example, the methyl resonance has a width of ~0.06 ppm. This is due in part to the slight inequivalence of the 20 different leucines within the peptide as well as to the unresolved J-couplings. Therefore, we expect this to set the lower limit on the accessible resolution for this peptide.

^{1}H MAS spectra of the peptide-20/DMPC-d_{54} mixture were taken as a function of spinning rate at two temperatures, 30 and 50°C. Below a spinning rate of 5 kHz, there is essentially no observable peptide signal at either temperature. At 30°C spinning at 6.5 kHz, one begins to see a broad peak, due to the peptide leucine methyls, underneath the lipid methyl and methylene resonances near 1.0 ppm. As the spinning rate increases, this peak sharpens and eventually dominates the much smaller lipid methyl peak. At higher spin rates, the peptide methylene resonances near 2.0 ppm also become visible. The peptide C-α ^{1}H peak lies beneath the lipid headgroup and glycerol backbone resonances (because the headgroup and backbone have not been deuterated), so it is difficult to extract unambiguously. Fig. 4 shows the spectra at 50°C for spinning rates from 8.0 to 14.0

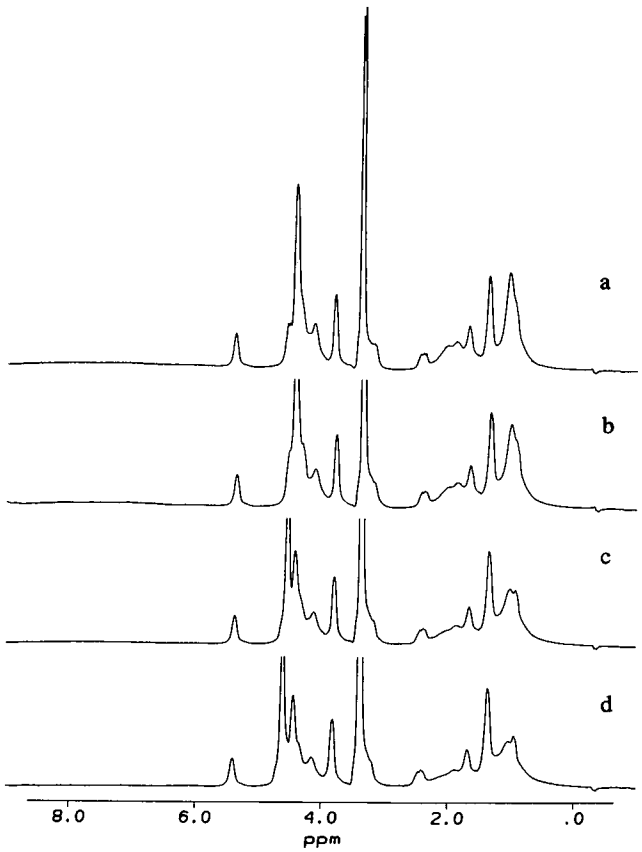

FIGURE 4 ^{1}H-MAS-NMR spectra of the peptide-20/DMPC-d_{54} mixture at 50°C; at spinning rates of (*a*) 14.0 kHz, (*b*) 12.0 kHz, (*c*) 10.0 kHz, and (*d*) 8.0 kHz. Note the dramatic increase in intensity of the peptide resonances near 1.0 and 2.0 ppm as spinning rate increases.

kHz. At this temperature, the peptide-20 resonances are even sharper. At the highest spinning rate, 14 kHz, the spectrum of Fig. 4 *a* shows a very strong leucine methyl peak and the two peptide methylene peaks, as well as increased intensity in the region near 4 ppm, where the C-α ^{1}H resonances are found. The use of headgroup-deuterated lipid would allow the unambiguous identification and quantification of this peptide resonance. Fig. 5 shows the spectrum from Fig. 4 *a*, at 14 kHz and 50°C on a twice-expanded vertical scale. There is a very broad peak with a maximum at ~8 ppm, corresponding to the expected position of the peptide-20 N-^{1}H resonances. However, the integrated area of this peak is much too large to be due simply to the amide hydrogens. It is likely that part of this peak is due to the background signal from the Vespel end caps used with this rotor. Nonetheless, the amide ^{1}H peak is clearly still very broad because it cannot be isolated readily from the background.

By simulating these spectra, we can extract the intensities, chemical shifts, and linewidths of at least the peptide-20 methyl and methylene resonances. Fig. 6 shows a comparison of the experimental spectrum at 50°C, at a spinning rate of 8.0 kHz (*top*), with the simulated spectrum (*middle*), and with the contributions of the peptide-20 resonances at 1.0, 1.9, 2.0, and 3.2 ppm (*bottom*). A comparison of the area of the lipid resonance at 5.3 ppm, which corresponds to the single glycerol C-2 ^{1}H per lipid, to the area of the peptide-20 leucine methyl resonance (which corresponds to 120 methyl ^{1}Hs per peptide), gives the ratio of 5.73 ± 1.4, whereas the theoretical value would be ~7.6 ± 0.2 (the uncertainty in this latter value is due to the 0.3 mol% uncertainty in the sample peptide concentration). Thus, we are seeing approximately the right relative signal intensities for the two components even though it is difficult to obtain the correct integrated intensities from the simulation of overlapping peaks. The simulation for the spectrum obtained at a rotation rate of 14 kHz is shown in Fig. 7.

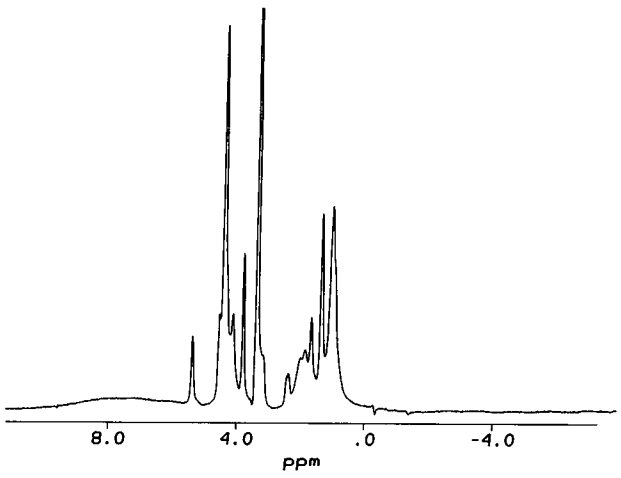

FIGURE 5 The ^{1}H-MAS-NMR spectrum of peptide-20/DMPC-d_{54} at 50°C at a spinning rate of 14 kHz (as in Fig. 4 *a*), on a twice-expanded vertical scale to show the broad feature near 8.0 ppm.

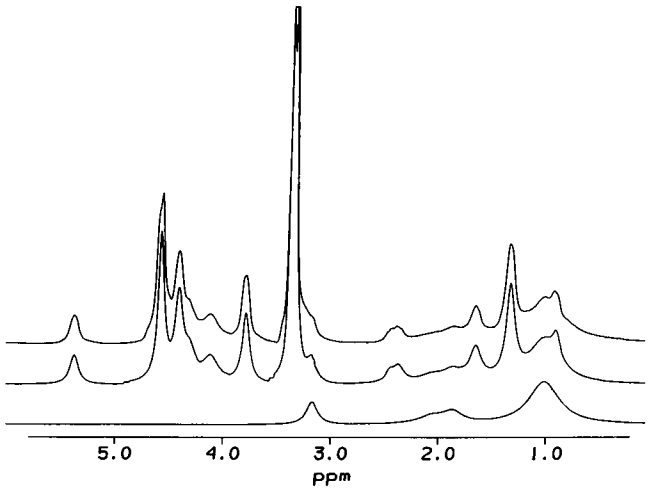

FIGURE 6 A comparison of the ^{1}H-MAS-NMR spectrum of the peptide-20/DMPC-d_{54} sample at 50°C, at a spinning rate of 8.0 kHz (*top*) with its simulation (*middle*). Three components of the simulation arising from peptide-20 are shown in the bottom trace. The simulation parameters for selected peaks are: for the lipid peak at 5.37 ± 0.01 ppm, area = 1.0, width = 34 ± 3 Hz; for the peptide leucine methyl peak at 1.01 ± 0.01 ppm, area = 5.40 ± 1.3, width = 126 ± 13 Hz; for the peptide methylene peak at 1.86 ± 0.02 ppm, area = 0.87 ± 0.22, width = 78 ± 8 Hz; for the peptide methylene peak at 2.04 ± 0.02 ppm, area = 0.78 ± 0.22, width = 106 ± 11 Hz. The intensities are normalized to the lipid peak at 5.37 ppm, and errors are estimated from the quality of the fit of the simulated to the experimental spectrum.

Comparison of the bottom traces of Figs. 6 and 7, which are the simulated peptide-20 resonances, shows how dramatically these peaks have sharpened due to the increased spinning rate. The linewidth of the peptide-20 methyl resonance is plotted as a function of spinning rate in Fig. 2, where the open circles refer to the spectra at 30°C, whereas the open squares are for the spectra at 50°C. Although the peptide-20 methyl resonance is considerably broader than the lipid resonances (also shown in Fig. 2), the dependence of the width on spinning rate is considerably more dramatic. Increasing the spinning rate from 6.5 to 14 kHz, a little more than a factor of two, has decreased the peptide-20 methyl linewidth from ~0.6 to 0.28 ppm, at 30°C, whereas at 50°C the linewidth at 14 kHz is only 0.18 ppm.

DISCUSSION AND CONCLUSIONS

To observe the high resolution ^{1}H-NMR spectra of either peptides or lipids in an ordered system such as a model or biological membrane, it is absolutely necessary to have rapid axially symmetric molecular reorientation. This modifies the character of the dipolar broadening of the spectra by projecting the interaction onto the axis of reorientation. MAS then can narrow effectively this residual "inhomogeneous" broadening. We have demonstrated that it is possible to observe the ^{1}H-NMR spectra of both lipids and peptides in the fluid phase of model membrane systems. In addition, we have found that the lipid linewidths correspond well

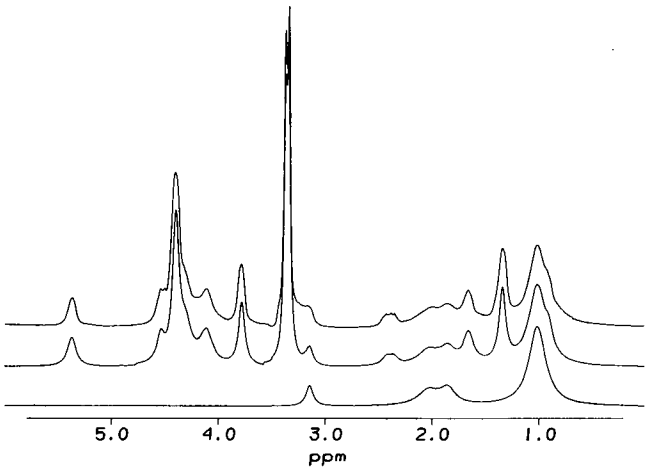

FIGURE 7 A comparison of the ^{1}H-MAS-NMR spectrum of the peptide-20/DMPC-d_{54} sample at 50°C, at a spinning rate of 14.0 kHz (*top*) with its simulation (*middle*). Three components of the simulation arising from peptide-20 are shown in the bottom trace. The simulation parameters for selected peaks are: for the lipid peak at 5.37 ± 0.01 ppm, area = 1.0, width = 34 ± 3 Hz; for the peptide leucine methyl peak at 1.01 ± 0.01 ppm, area = 5.41 ± 1.22, width = 68 ± 7 Hz; for the peptide methylene peak at 1.86 ± 0.02 ppm, area = 0.90 ± 0.23, width = 60 ± 6 Hz; for the peptide methylene peak at 2.04 ± 0.02 ppm, area = 1.38 ± 0.34, width = 87 ± 9 Hz. The intensities are normalized to the lipid peak at 5.37 ppm, and errors are estimated from the quality of the fit of the simulated to the experimental spectrum.

with the spectral densities measured both by field-cycling T_1 measurements at low frequencies and by $T_{1\rho}$, spin-lattice relaxation in the rotating frame, measurements. These linewidths change only slightly with increasing spinning rate, reflecting the rather flat frequency dependence of the spectral density in the 10–100 kHz range. This broad distribution of correlation times is characteristic of lipid bilayers, and to obtain any dramatic improvement, or reduction, in lipid linewidths it will be necessary to find conditions under which the amplitudes of these slow motions are reduced. It is likely that changes in sample composition, for example, changes in hydration level, incorporation of cholesterol, etc., although they may not cause these motions to become faster, will reduce their amplitudes and, hence, their effectiveness in broadening the lines.

At low spinning rates, the peptide resonances are too broad to detect, appearing only at rates above ~5 kHz. Further increases in spinning rate result in a dramatic decrease in the linewidths. Probably the most significant slow motions in the case of the peptides involve the reorientation of the diffusion (helix) axis either by a "wobbling" relative to the local bilayer normal (Prosser et al., 1994; Prosser and Davis, 1994) or by fluctuations in the orientation of the local bilayer normal itself. These latter motions can arise either through undulations in the bilayer surface (Bloom and Evans, 1991) or by diffusion of the peptide over the curved surface of the liposomes. For gramicidin A in oriented bilayers of DLPC, Prosser and Davis (1994) interpreted their relaxation data in terms of rapid axial diffusion of the peptide and a "wobbling" of the diffusion axis in the orienting potential of the bilayer. They arrived at a correlation time, $\tau_\perp$. For this "wobbling" motion of $\sim 6 \times 10^{-6}$ s. Over such long time scales, it is quite possible that both diffusion and surface undulations may also play an important role in the slow modulation of the residual proton dipolar second moment, resulting in contributions to the linewidth.

To use Eq. 35 to calculate the contribution of slow motions to the linewidth, we need to estimate the mean squared strength of the residual dipolar interaction which is modulated by this motion, i.e., ΔM_2. We use the proton second moments of dry powdered myoglobin at room temperature and of rhodopsin in DMPC at low lipid/protein ratio, which are in the range of 5 to 6 $\times$ 10^9 s^{-2}, as estimates of typical protein rigid lattice second moments ("rigid" except that there will be rapid methyl group reorientation at room temperature) (MacKay et al., 1983). The rapid reorientation of the peptide about the bilayer normal is expected to reduce the intramolecular contribution (which should be much larger than the intermolecular contribution) to the total second moment by roughly a factor of four. Thus, we estimate a residual peptide second moment of $\sim 1.25\text{–}1.5 \times 10^9$ s^{-2}. Of this, only ~10–15% can be attributed to the methyl group resonances on which we focus our discussion. Thus, the maximum available mean-squared interaction strength should be approximately in the range of

$$1.25 \times 10^8\ s^{-2} \leq \Delta M_2^{CH_3} \leq 2.25 \times 10^8\ s^{-2} \qquad (36)$$

To estimate the contribution of homogeneous broadening to the linewidth, from Eq. 34, we use a similar approach, starting with the residual methyl group second moment. The ^{1}H nuclei within a particular leucine side chain make by far the largest contribution to the dipolar second moment of the leucine methyl ^{1}H resonance. Because there is no contribution to the MAS linewidth due to interactions among the equivalent methyl ^{1}H nuclei, we need only consider the contribution of the dipolar interaction of the methyl ^{1}H with nonmethyl ^{1}H to the methyl group second moment. Within a leucine side chain, the four nonmethyl ^{1}H nuclei contribute only ~4% of the total second moment, the rest arising from interactions among the six methyl ^{1}H nuclei. Thus, the maximum contribution, $\delta M_2^{CH_3}$, from nonmethyl protons to the methyl second moment is in the range

$$5.0 \times 10^6 s^{-2} \leq \delta M_2^{CH_3} \leq 9.0 \times 10^6 s^{-2} \qquad (37)$$

Taking the square root of $\delta M_2^{CH_3}$ and dividing by 2π, and using an isotropic chemical shift difference of 1 ppm ~ 360 Hz, we estimate the contribution to the linewidth of the leucine methyl ^{1}H resonance to be

$$\Delta\nu_H \approx k_5(k_1 - k_2)/\nu_R \approx 360 \times \sqrt{\delta M_2^{CH_3}}/(2\pi \times \nu_R) \qquad (38)$$

or, at ν_R = 10 kHz,

$$13\ \text{Hz} \leq \Delta\nu_H \leq 17\ \text{Hz} \qquad (39)$$

Although this cannot account for the observed linewidth at 30°C of 145 Hz, it is an important contribution. The contribution of homogeneous broadening to the linewidths of the nonmethyl resonances can be analyzed in a similar fashion, using instead the full residual second moment. This leads to predicted contributions that may range from three to 10 times as large as those for the methyl peak. In some cases, this may dominate the observed linewidth.

Fig. 8 shows a comparison of the predictions of Eq. 35 with the experimental data obtained for peptide-20 at 30°C. The two parameters in Eq. 35, namely, the correlation time, $\tau_\perp$, and the mean-square interaction strength, $\Delta M_2^{CH_3}$,were adjusted to optimize the agreement with the experimental data. At 30°C the linewidths were measured for spinning rates ranging from 6.5 to 14.0 kHz, as given in Fig. 2, and the optimal values for the two parameters are $\tau_\perp = 1.6 \times 10^{-5}$ s and $\Delta M_2^{CH_3} = 1.45 \times 10^8$ s^{-2}. These values are close to those estimated above. The value of $\Delta M_2^{CH_3}$ suggests that a large fraction of the available second moment is being modulated by the slow motion. Although this is somewhat larger than expected from a comparison with gramicidin A in oriented bilayers of DLPC (Prosser and Davis, 1994), the difference may be related either to a lower orienting potential for the DMPC-d_{54}/peptide-20 bilayers or to differences in the dynamics in oriented and multilamellar dispersions. In any case, the estimates given above were only intended to give a rough idea of the order of magnitude expected, so in fact the agreement between these estimates and the fitted values is quite good. Moreover, the agreement between the experimental values for the linewidths and Eq. 24 is excellent. We conclude that the dominant cause of line broadening in the peptide-20 ^{1}H-NMR lines is most likely the fluctuations in the orientation of the diffusion (helix) axis.

Raising the temperature to 50°C, we might expect changes in the correlation times, the strength of the orienting potential, the lateral diffusion rates, and the amplitudes and frequencies of surface undulations. It is not clear a priori which of these will dominate. Fig. 9 shows the fit to the data at 50°C for rotation rates from 8.0 to 14.0 kHz. The best values for the two parameters at this temperature are $\tau_\perp = 1.6 \times 10^{-5}$ s and $\Delta M_2^{CH_3} = 0.97 \times 10^8$ s^{-2}. Clearly, we could make further small adjustments to these two parameters without changing the fit significantly (as one can see

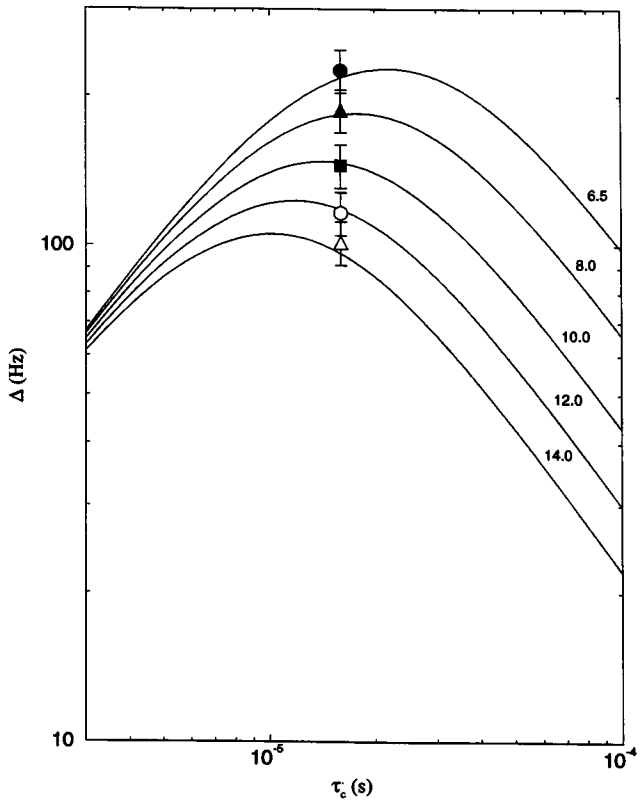

FIGURE 8 Comparison of the experimental spin-rate dependence of the peptide leucine methyl peak linewidth to the prediction of Eq. 24 in the text. T = 30°C at spinning rates: (●) 6.5 kHz, (▲) 8.0 kHz, (■) 10.0 kHz, (○) 12.0 kHz, and (△) 14.0 kHz. The set of theoretical curves were adjusted horizontally and vertically to match the experimental data; this resulted in the choice of the two parameters in Eq. 24: $\tau_c = 1.6 \times 10^{-5}$ s, and $\Delta M_2^{CH3} = 1.45 \times 10^8$ s^{-2}. The theoretical curves are labeled by the corresponding spinning rate.

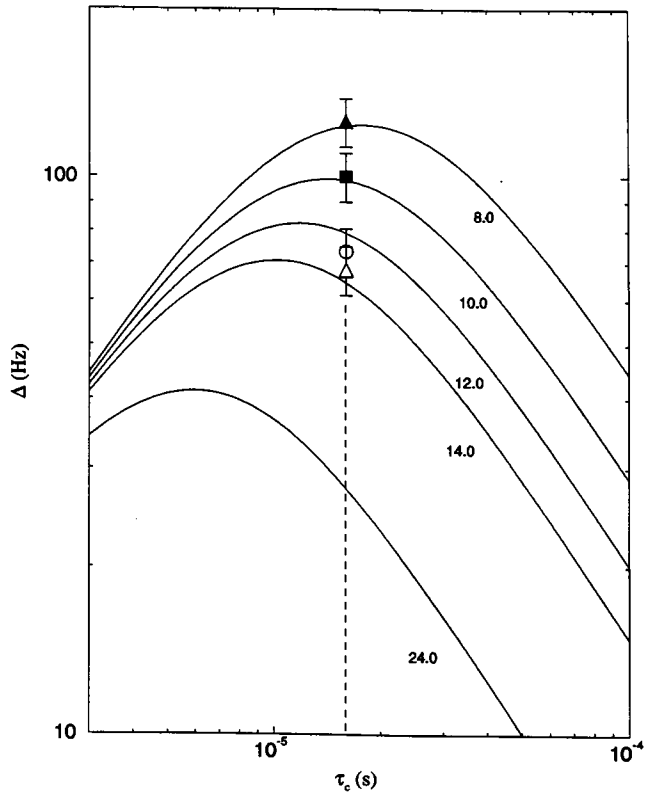

FIGURE 9 Comparison of the experimental spin-rate dependence of the peptide leucine methyl peak linewidth to the prediction of Eq. 24 in the text. T = 50°C at spinning rates: (▲) 8.0 kHz, (■) 10.0 kHz, (○) 12.0 kHz, and (△) 14.0 kHz. The set of theoretical curves were adjusted horizontally and vertically to match the experimental data; this resulted in the choice of the two parameters in Eq. 24: $\tau_c = 1.6 \times 10^{-5}$ s and $\Delta M_2^{CH3} = 0.97 \times 10^8$ s^{-2}. The theoretical curves are labeled by the corresponding spin rate. The curve labeled 24.0 and the vertical dashed line indicate the improvement in linewidth that is to be expected by spinning at this rate.

by simply displacing either the data points, as a block, or the fitted curves relative to each other in either direction), so one cannot take the fitted values of these two parameters too seriously. In fact, the two parameters are not completely independent. For such a complex dynamical system, it is quite plausible that an increase in temperature can result in a reduction in the fraction of the total mean-squared interaction strength available at low frequencies. For example, the residual quadrupolar splittings in a ^{2}H-NMR spectrum generally decrease as temperature is increased, reflecting the reduction in the order of the system. Because T_2 in ordered systems is dominated by fluctuations at low frequencies, an increase in amplitude and rate of rapid motions can result in a reduction in the effectiveness of the remaining slow fluctuations by bleeding some of the spectral density from the slow motion regime. This seems to be the case here. The correlation time for reorientation of the diffusion axis within the orienting potential of the bilayer may be quite insensitive to temperature; however, changes in the higher frequency motions may reduce the effectiveness of this slower motion in broadening the lines.

It will be interesting to investigate experimental methods for modifying both the correlation time, $\tau_\perp$, and $\Delta M_2^{CH_3}$. Clearly, these quantities are dependent on temperature, but they will also depend on composition. Preliminary experiments suggest that although cholesterol tends to increase the correlation times for lipid reorientation (Weisz et al., 1992), it leads to a sharpening of the peptide ^{1}H resonances, perhaps because of a significant increase in the strength of the orienting potential, and greatly stiffens the bilayer leading perhaps to a reduction in the importance of surface undulations. The difficulty with incorporating cholesterol in these systems is that cholesterol itself has a very complex ^{1}H spectrum that obscures that of the peptide. It is likely that changes in water concentration will also result in significant changes in both of these parameters, as may changes in the length of the phospholipid chains. Preliminary experiments have also shown that the peptide resonances are sharper for mixtures with lipids having shorter chains. Thus, the peptide linewidths follow the sequence DLPC < DMPC < DPPC. Changes in headgroup packing may also influence the strength of the orienting potential. Thus, there is considerable scope for improving the resolution of the peptide ^{1}H-NMR spectra by engineering changes in the molecular dynamics of the system through changes in composition. It is also possible to decrease the linewidths further by spinning faster, as suggested in Fig. 9. It is currently possible to spin samples at rates of up to 24–26 kHz. If the rate of decrease in linewidth as spinning rate increases can be extrapolated to 24 kHz, then a linewidth of ~26 Hz might be attainable simply by spinning more rapidly (although perhaps not with peptide-20 because this is close to the limiting linewidth, from solution measurements). It seems likely that, combining increases in spinning rate with slight changes in sample composition, it will be possible to reduce the linewidths by another factor of two or three.

One final question that arises in such high speed spinning experiments is the effect of the tremendous centripetal forces that occur in a sample spinning at such speeds. For 5-mm-diameter rotors, with internal diameters of 4 mm, spinning at 14 kHz, the centripetal acceleration at the inner surface is $\sim 1.5 \times 10^7$ m/s^2. Under the influence of this strong force, the sample coats the inner surface of the rotor to a depth of ~1 mm. At this depth, the pressure (assuming a density of 1 g/ml) is $\sim 2.6 \times 10^7$ Pa, or ~260 atmospheres. Assuming a typical isothermal compressibility of $\sim 10^{-9}$ m^2/N, such as those of water, benzene, dodecanol, etc., one estimates a change in volume of ~2.5%. The work done ($P\Delta V$) is $\sim 3.25 \times 10^5$ J/m^3. For a typical protein, of molecular weight 10^4, again assuming a density of ~1 gm/ml, this corresponds to $\sim 3.3 \times 10^3$ J/mole (or 0.78 kcal/mole). By comparison, the difference in free energy between the folded and unfolded states of a protein is estimated to be approximately in the range of 5–10 kcal/mole (Creighton, 1984). Thus, under this added hydrodynamic pressure we would expect the typical protein to retain its stable folded configuration. A potentially more serious problem may arise because of phase separation induced by these pressures. We have not noticed any changes in the NMR spectra that suggest any pressure-induced phase separations, at speeds up to 14.7 kHz and over a temperature range from −20 to +60°C.

Whether one will ever be able to obtain high resolution ^{1}H-NMR spectra from large membrane proteins in their native environment is uncertain. However, it should be possible to obtain such spectra for small peptides and protein fragments (for example, with molecular weights less than ~10,000). The only stringent requirement is that these molecules undergo rapid axially symmetric reorientation, meaning at a rate τ_c such that $M_2\tau_c^2 \ll 1$. Because the static M_2 for proteins is typically $\sim 5–6 \times 10^9$ s^{-2}, a correlation time $\tau_c \ll 1.3 \times 10^{-5}$ s is required. The small, synthetic bilayer-spanning peptide-20 and the natural pentadecapeptide gramicidin D dimer both reorient much more rapidly than this. Other peptides of similar molecular weight should have similar reorientational correlation times. Because one-dimensional, axial diffusion rates vary quite slowly with molecular weight, there may be quite a large range of peptides that satisfy this condition. Once high resolution spectra are obtainable, two-dimensional techniques can be used to simplify further and to assign the peaks in the spectra. Cross-peaks in ^{1}H-COSY experiments in gramicidin A/phospholipid/water mixtures have already been identified (Bouchard et al., 1995). In addition, that study has demonstrated that solid-state ^{1}H-NMR is sensitive to conformational changes in gramicidin A incorporated in lipid bilayers. Therefore, there seems to be considerable scope for the application of these powerful techniques at least to small membrane peptides, especially if used in conjunction with ^{15}N labeling.

The contribution of homogeneous broadening to the linewidth of different peaks in the ^{1}H spectrum depends on the fraction of the dipolar second moment of that peak, which is

due to nearby spins having different chemical shifts. In principle, especially for protons on the peptide backbone, this could make a substantial contribution to the total linewidth. This becomes even more important if the broadening due to slow motions can be reduced significantly. We are calculating second moments for each position on the peptide and hope to make comparisons with experiment in the near future.

The arguments presented here for dipolar broadening among abundant ^{1}H nuclei apply equally well to other abundant nuclei with strong dipole-dipole interactions. The use of completely ^{13}C-labeled peptides, using ^{1}H decoupling, should result in high resolution ^{13}C-MAS spectra because the strength of the ^{13}C-^{13}C dipolar coupling is much weaker than for the ^{1}H case, significantly relaxing the requirement for high speed spinning. Preliminary results on natural abundance ^{13}C and with specifically labeled peptides give linewidths of <1 ppm for carbonyl, α-carbon, and methyl carbon resonances. Although there is little homonuclear dipolar broadening for these preliminary experiments, high speed spinning should be capable of eliminating this as a broadening mechanism even for completely ^{13}C-labeled peptides.

This work was supported by a grant from the Natural Sciences and Engineering Research Council of Canada.

We thank Drs. Xi Shan and R. G. Griffin for many useful discussions and much practical guidance in the art of magic angle spinning. We also thank Drs. B. G. Nickel and Frances Sharom for many helpful discussions.

REFERENCES

Arseniev, A. S., A. L. Lomize, I. L. Barsukov and V. F. Bystrov. 1986. Gramicidin A transmembrane channel three-dimensional structure reconstruction based on NMR spectroscopy and conformational energy refinement. *J. Biol. Membr.* 3:1077–1104.

Bloom, M., E. E. Burnell, S. B. W. Roeder, and M. I. Valic. 1977. Nuclear magnetic resonance line shapes in lyotropic liquid crystals and related systems. *J. Chem. Phys.* 66:3012–3020.

Bloom, M., and E. Evans. 1991. Observation of surface undulations on the mesoscopic length scale by NMR. *In* Biologically Inspired Physics. L. Peliti, editor. Plenum Press, New York.

Bouchard, M., J. H. Davis, and M. Auger. 1995. High speed MAS solid-state ^{1}H-NMR study of the conformation of gramicidin A in lipid bilayers. *Biophys. J.* 69: In press.

Brink, D. M., and G. R. Satchler. 1993. Angular Momentum, 3rd. ed. Oxford University Press, Oxford, U.K.

Creighton, T. E. 1984. Proteins: Structures and Molecular Properties. W. H. Freeman, New York, 327 pp.

Creuzet, F., A. McDermott, R. Gebhard, K. van der Hoef, M. B. Spijker-Assink, J. Herzfeld, J. Lugtenburg, M. H. Levitt, and R. G. Griffin. 1991. Determination of membrane protein structure by rotational resonance NMR: bacteriorhodopsin. *Science.* 251:783–786.

Cowan, S. W., T. Schirmer, G. Rummel, M. Stiert, R. Ghosh, R. A. Pauptit, J. N. Jansonius, and J. P. Rosenbusch. 1992. Crystal structures explain functional properties of two *E. coli* porins. *Nature.* 358:727–733.

Datema, K. P., K. P. Pauls, and M. Bloom. 1986. Deuterium NMR investigations of the exchangeable sites on gramicidin A and gramicidin S in multilamellar vesicles of dipalmitoylphosphatidylcholine. *Biochemistry.* 25:3796–3803.

Davis, J. H., D. M. Clare, R. S. Hodges, and M. Bloom. 1983. Interaction of a synthetic amphiphilic polypeptide and lipids in a bilayer structure. *Biochemistry.* 22:5298–5305.

Davis, J. H. 1983. The description of membrane lipid conformation, order and dynamics by ^{2}H NMR. *Biochim. Biophys. Acta.* 737:117–171.

Davis, J. H. 1988. ^{2}H Nuclear magnetic resonance of exchange-labeled gramicidin in an oriented lyotropic nematic phase. *Biochemistry.* 27: 428–436.

Davis, J. H. 1991. Deuterium nuclear magnetic resonance spectroscopy in partially ordered systems. *In* Isotopes in the Physical and Biomedical Sciences, Vol. 2. E. Buncel and J. R. Jones, editors. Elsevier, Amsterdam. 99–157.

Davis, J. H. 1993. The molecular dynamics, orientational order and thermodynamic phase equilibria of cholesterol/phosphatidylcholine mixtures: ^{2}H nuclear magnetic resonance. *In* Cholesterol in Membrane Models. L. Finegold, editor. CRC Press, Boca Raton, FL. 67–135.

Deisenhofer, J., and H. Michel. 1989. The photosynthetic reaction center from the purple bacterium *Rhodopseudomonas viridis. Science.* 245: 1463–1473.

Forbes, J., C. Husted, and E. Oldfield. 1988. High-field, high-resolution proton "magic-angle" sample-spinning nuclear magnetic resonance spectroscopic studies of gel and liquid crystalline lipid bilayers and the effects of cholesterol. *J. Am. Chem. Soc.* 110:1059–1065.

Griffin, R. G. 1981. Solid state nuclear magnetic resonance of lipid bilayers. *Methods Enzymol.* 72:108–174.

Griffin, R. G., W. P. Aue, R. A. Haberkorn, G. S. Harbison, J. Herzfeld, E. M. Menger, M. G. Munowitz, E. T. Olejniczak, D. P. Raleigh, J. E. Roberts, D. J. Ruben, A. Schmidt, S. O. Smith, and S. Vega. 1988. Magic-angle sample spinning. *In* Physics of NMR Spectroscopy in Biology and Medicine. E. Fermi, editor. North-Holland, Amsterdam. 203–266.

Gupta, C. M., R. Radhakrishnan, and H. G. Khorana. 1975. Glycerophospholipid synthesis: improved general method and new analogs containing photoactivable groups. *Proc. Natl. Acad. Sci. USA.* 74:4315–4319.

Haeberlen, U. 1976. High resolution NMR in solids: selective averaging. *In* Advances in Magnetic Resonance. Academic Press, New York.

Haeberlen, U., and J. S. Waugh. 1968. Coherent averaging effects in magnetic resonance. *Phys. Rev.* 175:453–467.

Haeberlen, U., and J. S. Waugh. 1969. Spin-lattice relaxation in periodically perturbed systems. *Phys. Rev.* 185:420–429.

Henderson, R., and P. N. T. Unwin. 1975. Three dimensional model of purple membrane obtained by electron microscopy. *Nature.* 257:28–32.

Henderson, R., J. M. Baldwin, T. A. Ceska, F. Zemlin, E. Beckmann, and K. H. Downing. 1990. Model for the structure of bacteriorhodopsin based on high-resolution electron cryo-microscopy. *J. Mol. Biol.* 213: 899–929.

Henry, G. D., and B. D. Sykes. 1992. Assignments of amide ^{1}H and ^{15}N NMR resonances in detergent-solubilized M13 coat protein: a model for the coat protein dimer. *Biochemistry.* 31:5284–5297.

Hoult, D. I., and R. E. Richards. 1975. Critical factors in the design of sensitive high-resolution nuclear magnetic resonance spectrometers *Proc. R. Soc. Lond. A.* 344:311–340.

Huang, T. H., C. W. B. Lee, S. K. Das Gupta, A. Blume, and R. G. Griffin. 1993. A ^{13}C and ^{2}H nuclear magnetic resonance study of phosphatidylcholine/cholesterol interactions: characterization of liquid-gel phases. *Biochemistry.* 32:13277–13287.

Huschilt, J. C., R. S. Hodges, and J. H. Davis. 1985. Phase equilibria in an amphiphilic peptide-phospholipid model membrane by deuterium nuclear magnetic resonance difference spectroscopy. *Biochemistry.* 24: 1377–1386.

Karslake, C., M. E. Piotto, J. K. Pak, H. Weiner, and D. G. Gorenstein. 1990. 2D NMR and structural model for a mitochondrial signal peptide bound to a micelle. *Biochemistry.* 29:9872–9878.

Ketchem, R. R., W. Hu, and T. A. Cross. 1993. High-resolution conformation of gramicidin A in a lipid bilayer by solid-state NMR. *Science.* 261:1457–1460.

Kimmich, R., G. Schnur, and A. Scheuermann. 1983. Spin-lattice relaxation and lineshape parameters in nuclear magnetic resonance of lamellar lipid systems: fluctuation spectroscopy of disordering mechanisms. *Chem. Phys. Lipids.* 32:271–322.

Kohda, D., and F. Khagaki. 1992. Structure of epidermal growth factor bound to perdeuterated dodecylphosphocholine micelles determined by two-dimensional NMR and simulated annealing calculations. *Biochemistry*. 31:677–685.

Langlais, D. B. 1994. Internuclear distance measurements using rotational resonance. Ph.D. thesis. University of Guelph, Guelph, Ontario, Canada.

Le Guerneve, C., and M. Auger. 1995. New approach to study fast and slow motions in lipid bilayers: application to DMPC-cholesterol interactions. *Biophys. J.* 68:1952–1959.

Levitt, M. H., D. P. Raleigh, F. Creuzet, and R. G. Griffin. 1990. Theory and simulations of homonuclear spin pair systems in rotating solids. *J. Chem. Phys.* 92:6347–6364.

Long, J. R., B. Q. Sun, A. Bowen, and R. G. Griffin. 1994. Molecular dynamics and magic angle spinning NMR. *J. Am. Chem. Soc.* 116: 11950–11956.

Macdonald, P. M., and J. Seelig. 1988. Dynamic properties of gramicidin A in phospholipid membranes. *Biochemistry*. 27:2357–2364.

Maciel, G. E., C. E. Bronnimann, and B. L. Hawkins. 1990. High-resolution ^{1}H nuclear magnetic resonance in solids via CRAMPS. *Adv. Magn. Reson.* 14:125–150.

MacKay, A. L. 1981. A proton NMR moment study of the gel and liquid-crystalline phases of dipalmitoyl phosphatidylcholine. *Biophys. J.* 35:301–313.

MacKay, A. L., E. E. Burnell, A. Bienvenue, P. F. Devaux, and M. Bloom. 1983. Flexibility of membrane proteins by broad-line proton magnetic resonance. *Biochim. Biophys. Acta*. 728:460–462.

Maricq, M. M., and J. S. Waugh. 1979. NMR in rotating solids. *J. Chem. Phys.* 70:3300–3316.

McDermott, A. E., F. J. Creuzet, A. C. Kolbert, and R. G. Griffin. 1992. High resolution magic-angle-spinning spectra of protons in deuterated solids. *J. Magn. Reson.* 98:408–413.

McDermott, A. E., F. Creuzet, R. Gebhard, K. van der Hoef, M. H. Levitt, J. Herzfeld, J. Lugtenburg, and R. G. Griffin. 1994. Determination of internuclear distances and the orientation of functional groups by solid-state NMR: rotational resonance study of the conformation of retinal in bacteriorhodopsin. *Biochemistry*. 33:6129–6136.

Mehring, M. 1983. Principles of High Resolution NMR in Solids. Springer-Verlag, Berlin.

Oldfield, E., J. L. Bowers, and J. Forbes. 1987. High-resolution proton and carbon-13 NMR of membranes: why sonicate? *Biochemistry*. 26: 6919–6923.

Opella, S. J., P. L. Stewart, and K. G. Valentine. 1987. Protein structure by solid-state NMR spectroscopy. *Q. Rev. Biophys.* 19:7–49.

Orekhov, V. Yu., G. V. Abdulaeva, L. Yu. Musina, and A. S. Arseniev. 1992. ^{1}H-^{15}N-NMR studies of bacteriorhodopsin *Halobacterium halobium*. Conformational dynamics of the four-helical bundle. *Eur. J. Biochem.* 210:223–229.

Orekhov, V. Yu., K. V. Pervushin, and A. S. Arseniev. 1994. Backbone dynamics of (1–71)bacterioopsin studied by two-dimensional ^{1}H-^{15}N NMR spectroscopy. *Eur. J. Biochem.* 219:887–896.

Pascal, S. M., and T. A. Cross. 1992. Structure of an isolated gramicidin A double helical species by high-resolution nuclear magnetic resonance. *J. Mol. Biol.* 226:1101–1109.

Pauls, K. P., A. L. MacKay, O. Soderman, M. Bloom, A. K. Tanjea, and R. S. Hodges. 1985. Dynamic properties of the backbone of an integral membrane polypeptide measured by ^{2}H NMR. *Eur. Biophys. J.* 12:1–11.

Peersen, O. B., S. Yoshimura, H. Hojo, S. Aimota, and S. O. Smith. 1992. Rotational resonance NMR measurements of internuclear distances in an α-helical peptide. *J. Am. Chem. Soc.* 114:4332–4335.

Pervushin, K. V., V. Yu. Orekhov, A. I. Popov, L. Yu. Musina, and A. S. Arseniev. 1994. Three-dimensional structure of (1–71)bacterioopsin solubilized in methanol/chloroform and SDS micelles determined by ^{15}N-^{1}H heteronuclear NMR spectroscopy. *Eur. J. Biochem.* 219: 571–583.

Peters, A. R., N. Dekker, L. van den Berg, R. Boelens, R. Kaptein, A. J. Slotboom, and G. H. de Haas. 1992. Conformational changes in phospholipase A_2 upon binding to micellar interfaces in the absence and presence of competitive inhibitors. A ^{1}H and ^{15}N NMR study. *Biochemistry*. 31:10024–10030.

Picot, D., P. J. Loll, and R. M. Garavito. 1994. The x-ray crystal structure of the membrane protein prostaglandin H_2 synthase-1. *Nature*. 367: 243–249.

Pope, J. M., and B. A. Cornell. 1979. Pulsed NMR study of lipids, bound water and sodium ions in macroscopically-oriented lecithin/water lyotropic liquid crystal model membrane systems. *Chem. Phys. Lipids*. 24:27–43.

Prosser, R. S., J. H. Davis, C. Mayer, K. Weisz, and G. Kothe. 1992. Deuterium NMR relaxation studies of peptide-lipid interactions. *Biochemistry*. 31:9355–9363.

Prosser, R. S., S. I. Daleman, and J. H. Davis. 1994. The structure of an integral membrane peptide: a deuterium NMR study of gramicidin. *Biophys. J.* 66:1415–1428.

Prosser, R. S., and J. H. Davis. 1994. Dynamics of an integral membrane peptide: a deuterium NMR relaxation study of gramicidin. *Biophys. J.* 66:1429–1440.

Raleigh, D. P., M. H. Levitt, and R. G. Griffin. 1988. Rotational resonance in solid state NMR. *Chem. Phys. Lett.* 146:71–76.

Sanders, C. R. 1993. Solid state ^{13}C NMR of unlabeled phosphatidylcholine bilayers: spectral assignments and measurement of carbon-phosphorus dipolar couplings and ^{13}C chemical shift anisotropies. *Biophys. J.* 64:171–181.

Seelig, J., and A. Seelig. 1980. Lipid conformation in model membranes and biological membranes. *Q. Rev. Biophys.* 13:19–61.

Seelig, J. 1978. ^{31}P nuclear magnetic resonance and the head group structure of phospholipids in membranes. *Biochim. Biophys. Acta*. 505: 105–140.

Shan, X. 1990. High resolution nuclear magnetic resonance studies of lipids and model membranes. Ph.D. thesis. University of Illinois Champagne-Urbana, IL.

Shon, K., Y. Kim, L. Colnago, and S. J. Opella. 1991. NMR studies of the structure and dynamics of membrane-bound bacteriophage Pf1 coat protein. *Science*. 252:1303–1305.

Smith, R., D. E. Thomas, F. Separovic, A. R. Atkins, and B. A. Cornell. 1989. Determination of the structure of a membrane-incorporated ion channel. Solid-state nuclear magnetic resonance studies of gramicidin A. *Biophys. J.* 56:307–314.

Smith, S. O., J. Hamilton, A. Salmon, and B. J. Bormann. 1994a. Rotational resonance NMR determination of intra- and inter-molecular distance constraints in dipalmitoylphosphatidylcholine bilayers. *Biochemistry*. 33:6327–6333.

Smith, S. O., R. Jonas, M. Braiman, and B. J. Bormann. 1994b. Structure and orientation of the transmembrane domain of glycophorin A in lipid bilayers. *Biochemistry*. 33:6334–6341.

Sparling, M. L., R. Zidovetzki, L. Muller, and S. I. Chan. 1989. Analysis of membrane lipids by 500 MHz ^{1}H NMR. *Anal. Biochem.* 178:67–76.

Suwelack, D., W. P. Rothwell, and J. S. Waugh. 1980. Slow molecular motion detected in the NMR spectra of rotating solids. *J. Chem. Phys.* 73:2559–2569.

Thompson, L. K., A. E. McDermott, J. Raap, C. M. van der Wielen, J. Lugtenburg, J. Herzfeld, and R. G. Griffin. 1992. Rotational resonance NMR study of the active site structure in bacteriorhodopsin: conformation of the schiff base linkage. *Biochemistry*. 31:7931–7938.

Ulrich, A. S., M. P. Heyn, and A. Watts. 1992. Structure determination of the cyclohexene ring of retinal in bacteriorhodopsin by solid-state deuterium NMR. *Biochemistry*. 31:10390–10399.

van der Leeuw, Y. C. W., and G. Stulen. 1981. Proton relaxation measurements on lipid membranes oriented at the magic angle. *J. Magn. Reson.* 42:434–445.

Wang, D. N., W. Kuhlgrandt, V. E. Sarabia, and R. A. F. Reithmeier. 1993. Two-dimensional structure of the membrane domain of human Band 3, the anion transport protein of the erythrocyte membrane. *EMBO J.* 12:2233–2239.

Watts, A. 1988. Dynamic Properties of Biomolecular Assemblies. S. Harding, and A. J. Rowe, editors. Royal Chemical Society, London. 320–347.

Weisz, K., G. Grobner, C. Mayer, J. Stohrer, and G. Kothe. 1992. Deuteron nuclear magnetic resonance study of the dynamic organization of phospholipid/cholesterol bilayer membranes: molecular properties and viscoelastic behaviour. *Biochemistry*. 31:1100–1112.

Wennerstrom, H. 1973. Proton nuclear magnetic resonance lineshapes in lamellar liquid crystals. *Chem. Phys. Lett.* 18:41–44.

Wu, C. H., A. Ramamoorthy, and S. J. Opella. 1994. High-resolution heteronuclear dipolar solid-state NMR spectroscpy. *J. Magn. Reson.* 109:270–272.

Zare, R. N. 1988. Angular Momentum. Understanding Spatial Aspects in Chemistry and Physics. John Wiley & Sons, New York.

Zetta, L., R. Consonni, A. de Marco, R. Longhi, E. Manera, and G. Vecchio. 1990. Opiod peptides in micellar systems: conformational analysis by CD and by one-dimensional and two-dimensional ^{1}H-NMR spectroscopy. *Biopolymers.* 30:899–909.

Zheng, L., K. W. Fishbein, R. G. Griffin, and J. Herzfeld. 1993. Two-dimensional solid-state proton NMR and proton exchange. *J. Am. Chem. Soc.* 115:6254–6261.